

Electronic Supplementary/Supporting Information (ESI)

Synthesis of oxime-based CO-releasing molecules, CORMs and their immobilization on maghemite nanoparticles for magnetic-field induced CO release

Hajo Meyer,^a Markus Brenner,^a Simon Patrick Höfert,^a Tim Oliver Knedel,^a Peter Kunz,^a Annette M. Schmidt,^b Alexandra Hamacher,^c Matthias U. Kassack,^c Christoph Janiak^{a}*

^aInstitut für Anorganische Chemie und Strukturchemie, Universität Düsseldorf, 40204 Düsseldorf, Germany. Email: janiak@uni-duesseldorf.de

^bInstitut für Physikalische Chemie, Universität zu Köln, Luxemburger Str. 116, D-50939 Köln, Germany. Email: annette.schmidt@uni-koeln.de

^cInstitut für Pharmazeutische und Medizinische Chemie, Universität Düsseldorf, 40204 Düsseldorf, Germany. Email: matthias.kassack@hhu.de

hajo.meyer@uni-duesseldorf.de

markus.brenner1@rwth-aachen.de

Simon-Patrick.Hoefert@uni-duesseldorf.de

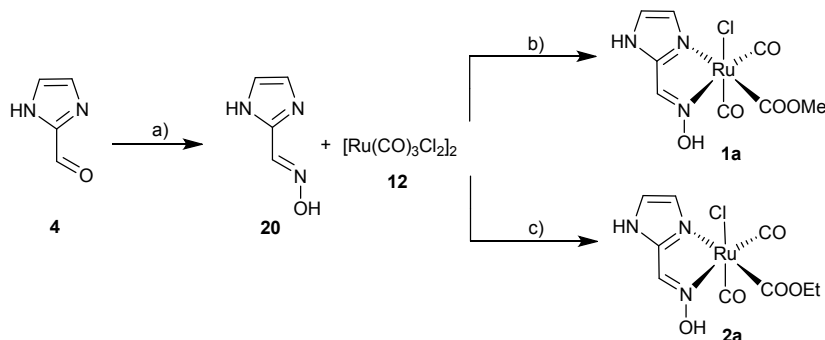
Tim-Oliver.Knedel@uni-duesseldorf.de

dr.peter.kunz@gmail.com

alexandra.hamacher@hhu.de

Synthesis of oxime-CORMs

In a first step following the literature,¹ imidazole-2-carboxaldehyde (**4**) was transformed to imidazole-2-carbaldehyde-oxime (**20**) with hydroxylamine hydrochloride and sodium carbonate in water. The reaction time was extended to 24 h at 70 °C to form product **2** with a yield of 41 %. A ¹H-NMR spectrum of imidazole-2-carbaldehyde-oxime (**20**) could not be recorded, not even in DMSO-d₆ due to very low solubility. Instead, a mixture of NaOD-D₂O was used to deprotonate the oxime in order to achieve solubility.



Scheme S1 Synthesis of the oxime-based CORMs Ru(imidazole-2-carbaldehyde-oxime)(methoxycarbonyl)(CO)₂Cl (**1a**) and Ru(imidazole-2-carbaldehyde-oxime)(ethoxycarbonyl)(CO)₂Cl (**2a**) starting from imidazole-2-carboxaldehyde (**4**) over imidazole-2-carbaldehyde-oxime (**20**). a) NH₂OH·HCl, Na₂CO₃, H₂O, 24 h, 70 °C; b) MeOH, 5 d, 30 °C; c) EtOH, 5 d, 30 °C.

The tricarbonyldichloridoruthenium dimer (**12**) was synthesized in a steel autoclave with glass-inlet according to a known procedure of Mantovani.² To form the oxime-based CORMs **1a** and **2a** the reaction conditions, as described by Oresmaa,¹ were modified to 30 °C and 5 d. Otherwise, only a very small amount of product was formed for both (**1a** and **2a**). We were able to receive 31 % yield for **1a** and 45 % yield for **2a**, which is only slightly less than the literature values (41 % and 53 %, respectively).

Synthesis of imidazole-2-carbaldehyde-oxime (20): 1.44 g (20.7 mmol) NH₂OH·HCl were dissolved in 8 mL of d.d. water and neutralized with 1.1 g (10.4 mmol) Na₂CO₃. Afterwards 1.0 g (10.4 mmol) imidazole-2-carboxaldehyde (**4**) was added and the solution was stirred for 24 h at 70 °C. After cooling with ice a colorless solid was sedimented, filtered and washed with d.d. water. The solid was dried under vacuum. Yield: 478 mg (41 %, Lit.: 44 %¹). IR (KBr): $\tilde{\nu}$ [cm⁻¹] = 3193, 3034, 2949, 930, 984. ESI-MS: m/z = 112.05 [M+H]⁺. ¹H-NMR (300 MHz, NaOD/D₂O): δ [ppm] = 6.78 (s, 1H, C-CH=N), 6.39 (s, 2H, imi-CH=CH).

^1H and ^{13}C NMR Spectra

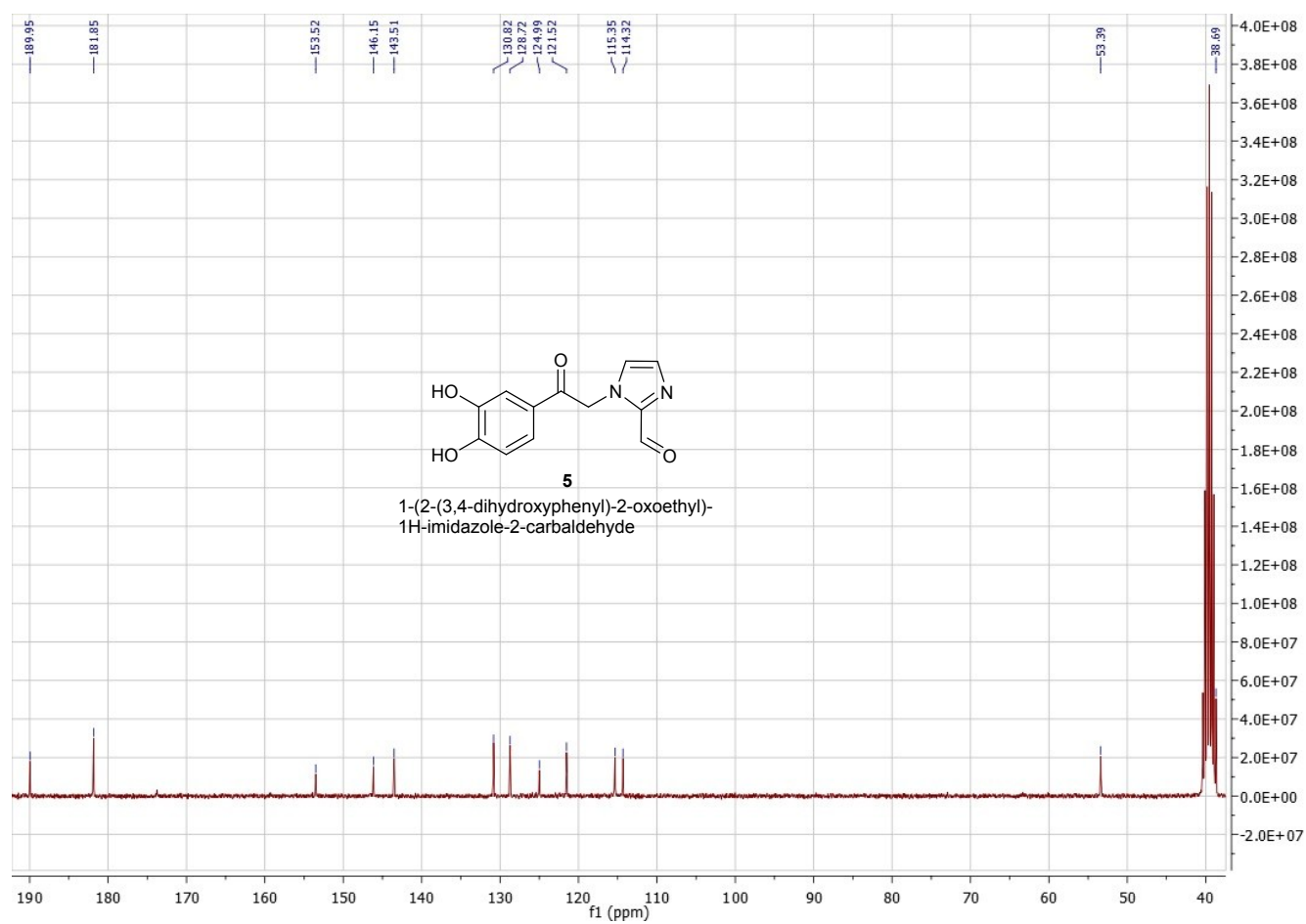


Fig. S1a ^{13}C NMR spectrum (75 MHz, DMSO-d_6) of 1-(2-(3,4-dihydroxyphenyl)-2-oxoethyl)-1H-imidazole-2-carbaldehyde, **5**.

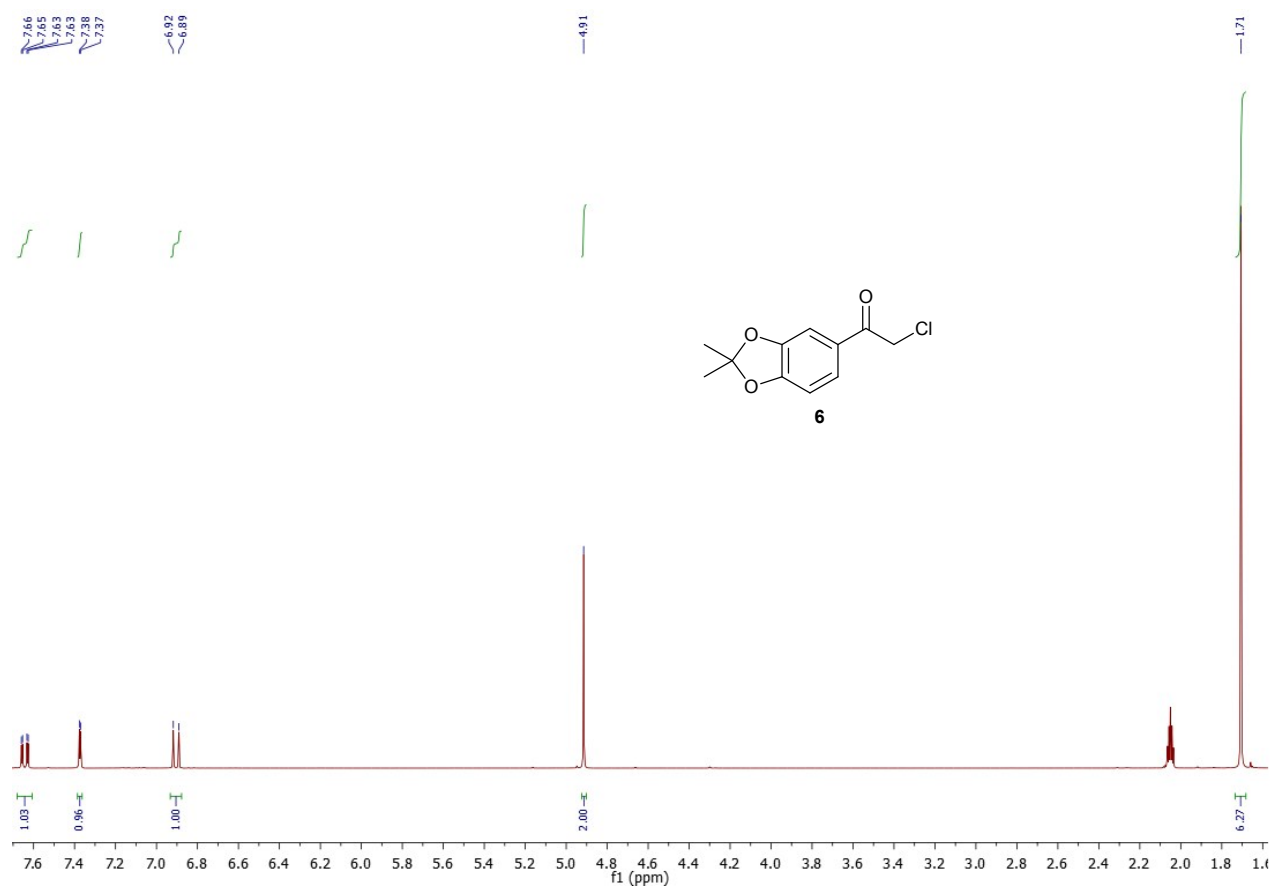
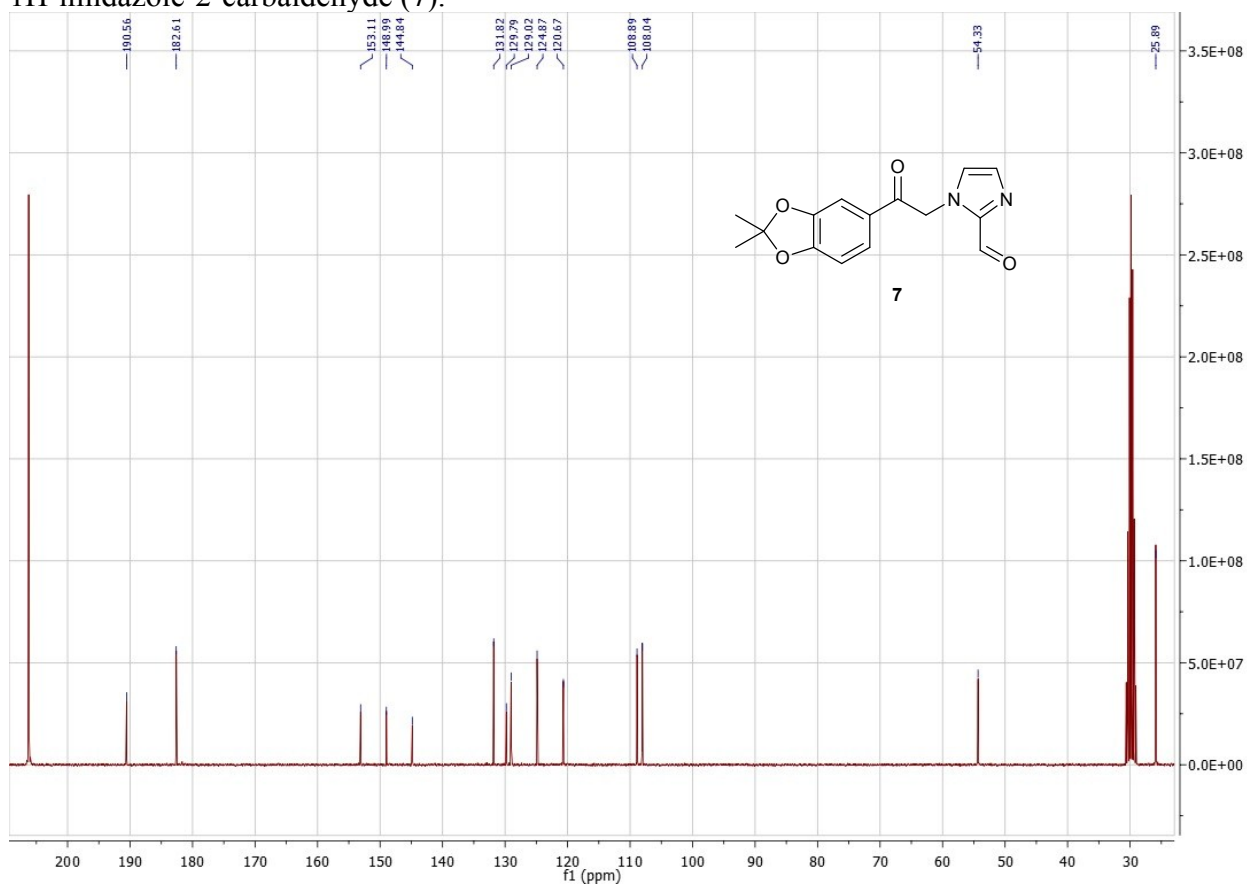
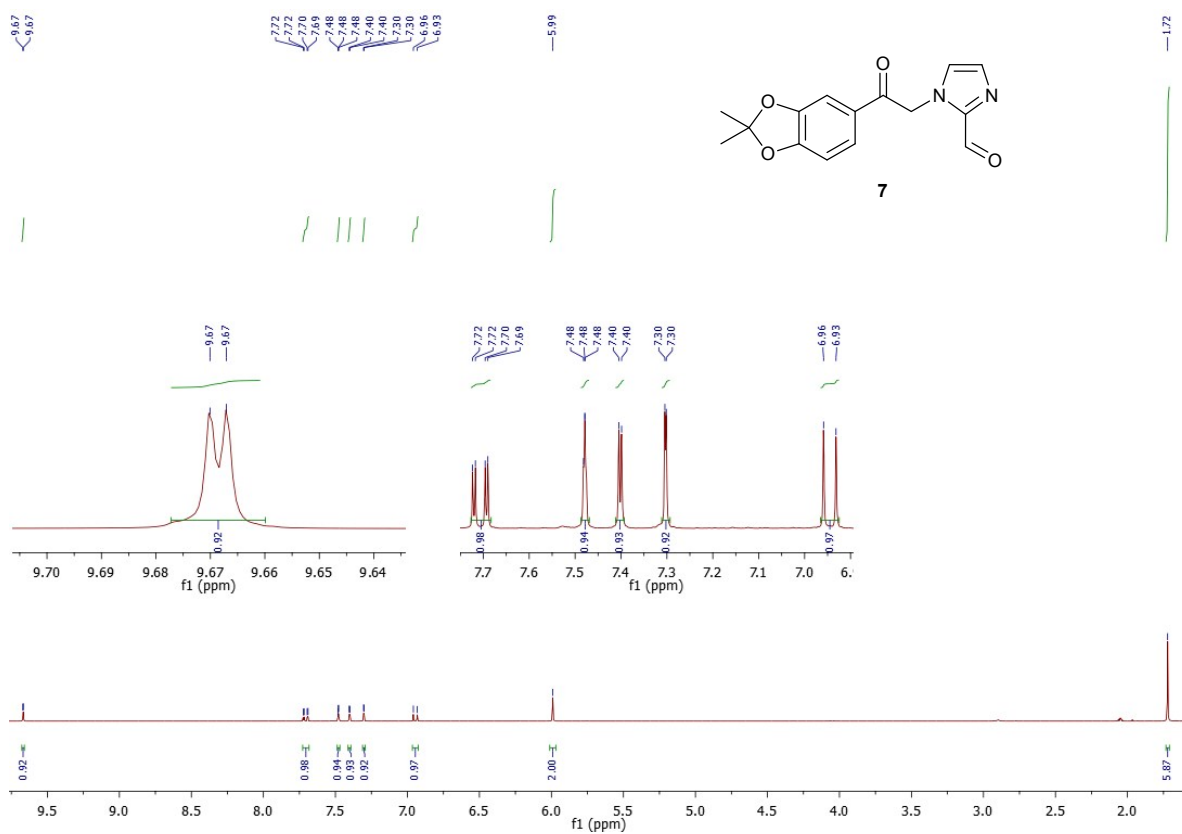


Fig. S1b ¹H NMR (300 MHz, acetone-d₆) of 2-chloro-1-(2,2-dimethylbenzo[d][1,3]dioxol-5-yl)ethanone (**6**)



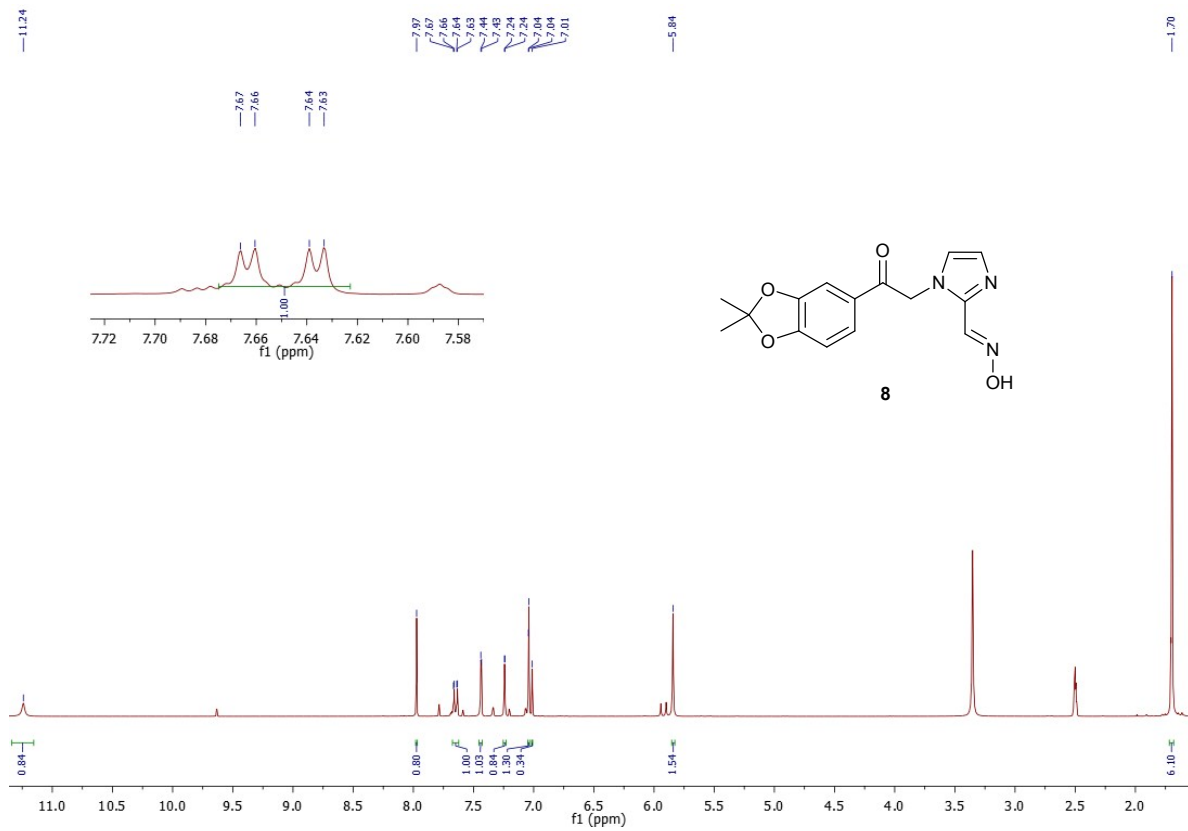
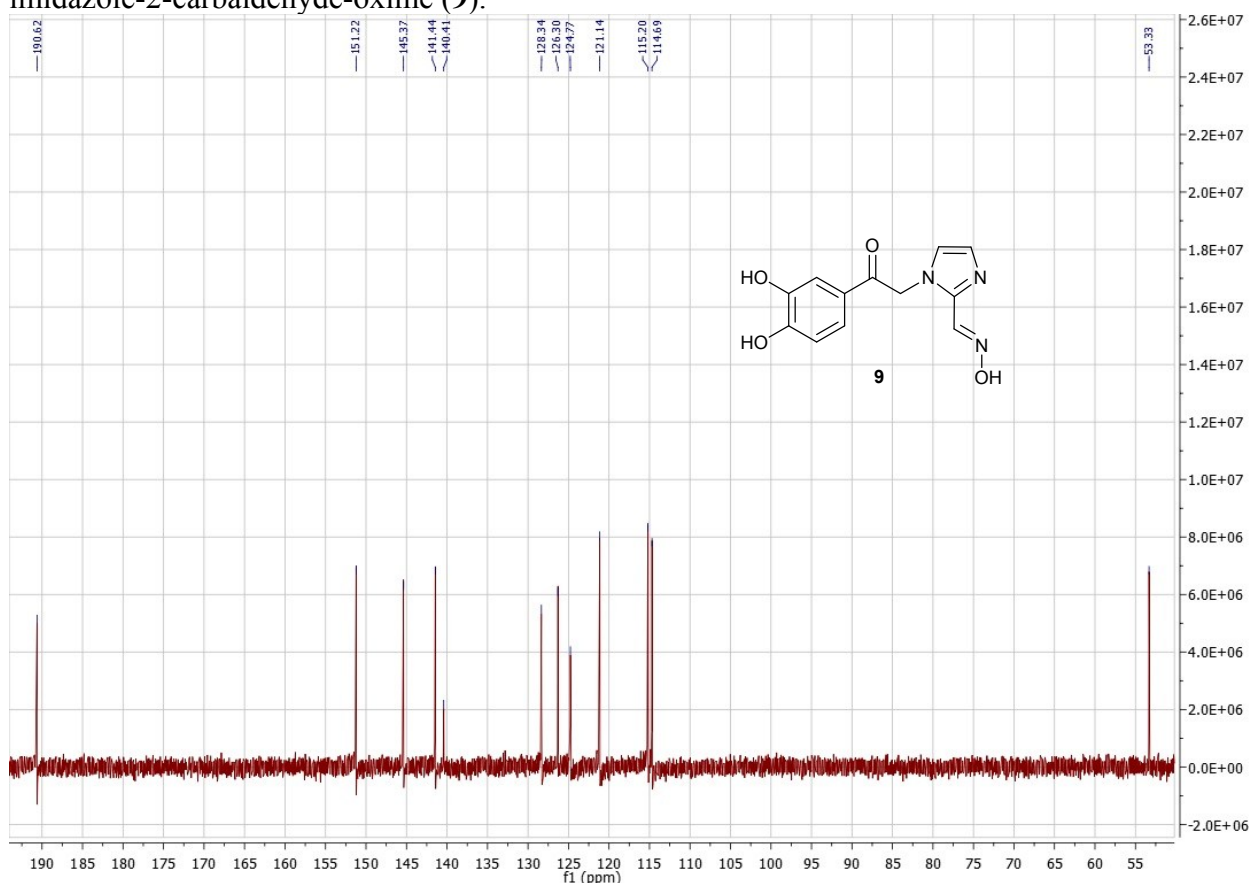
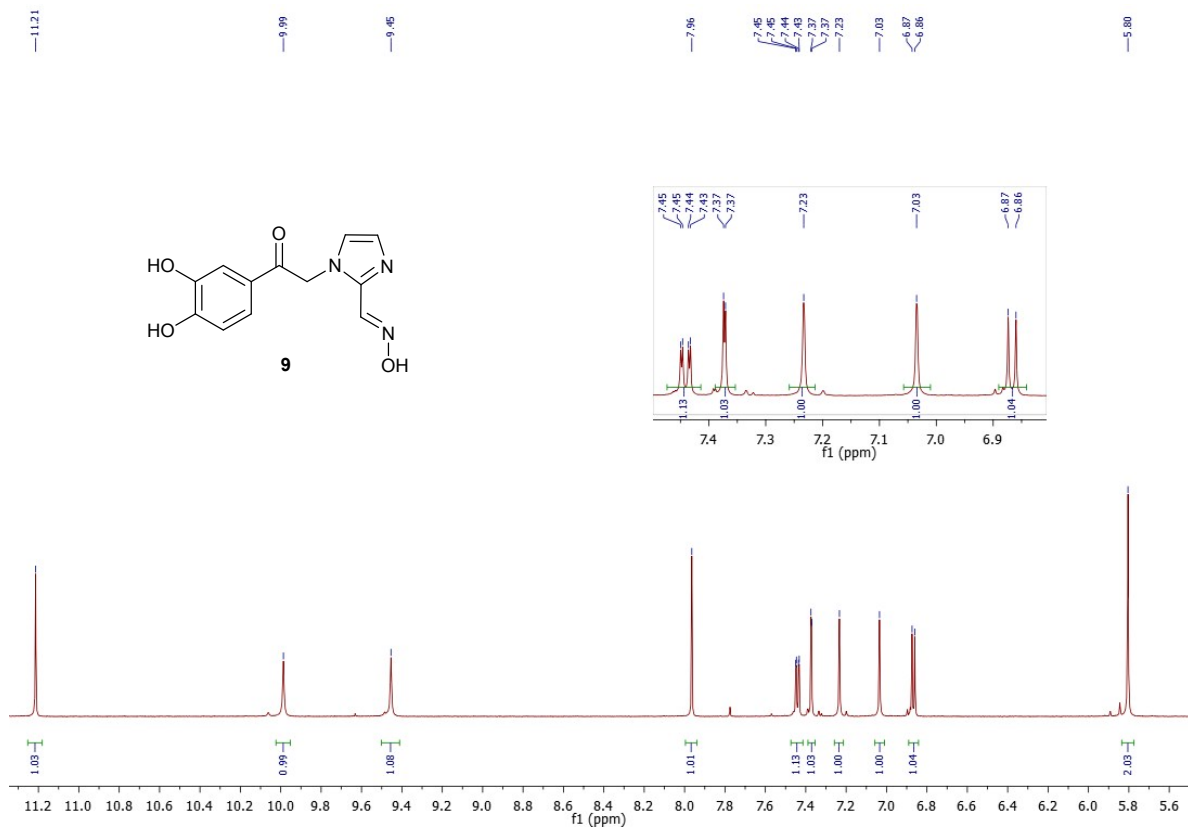
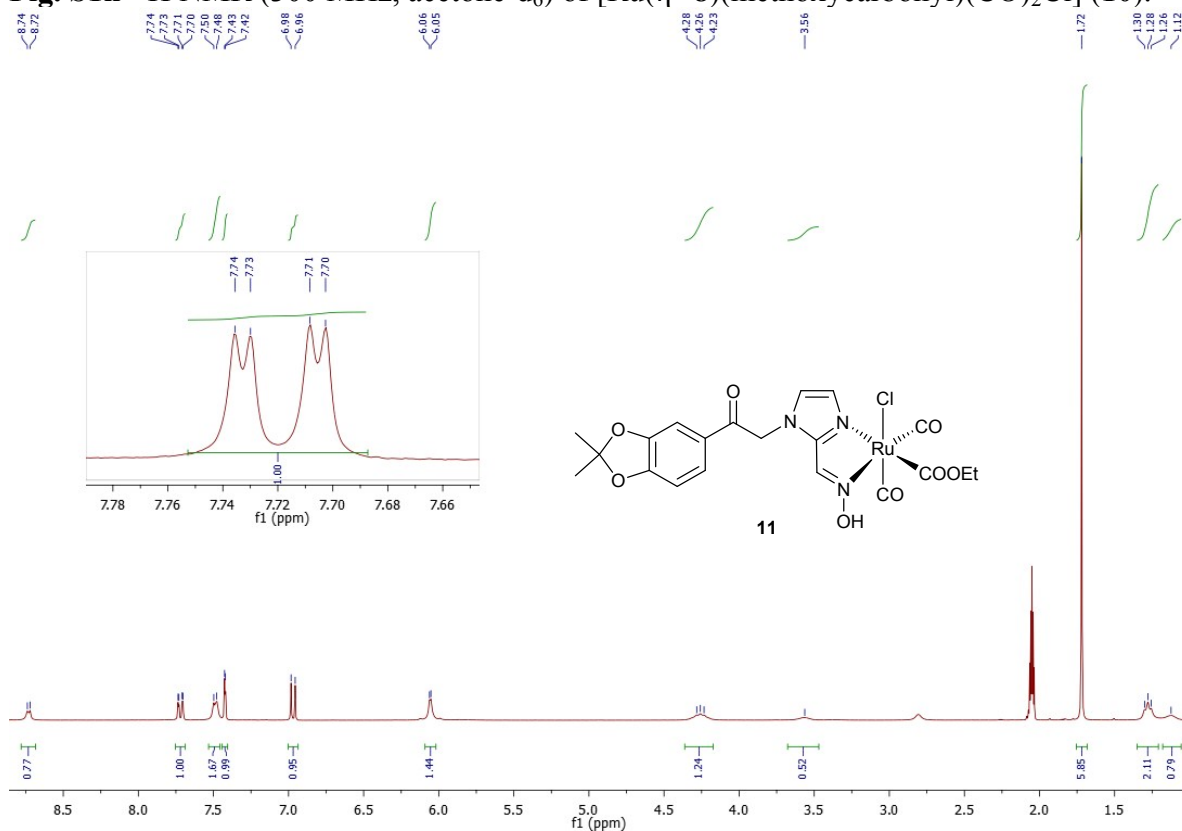
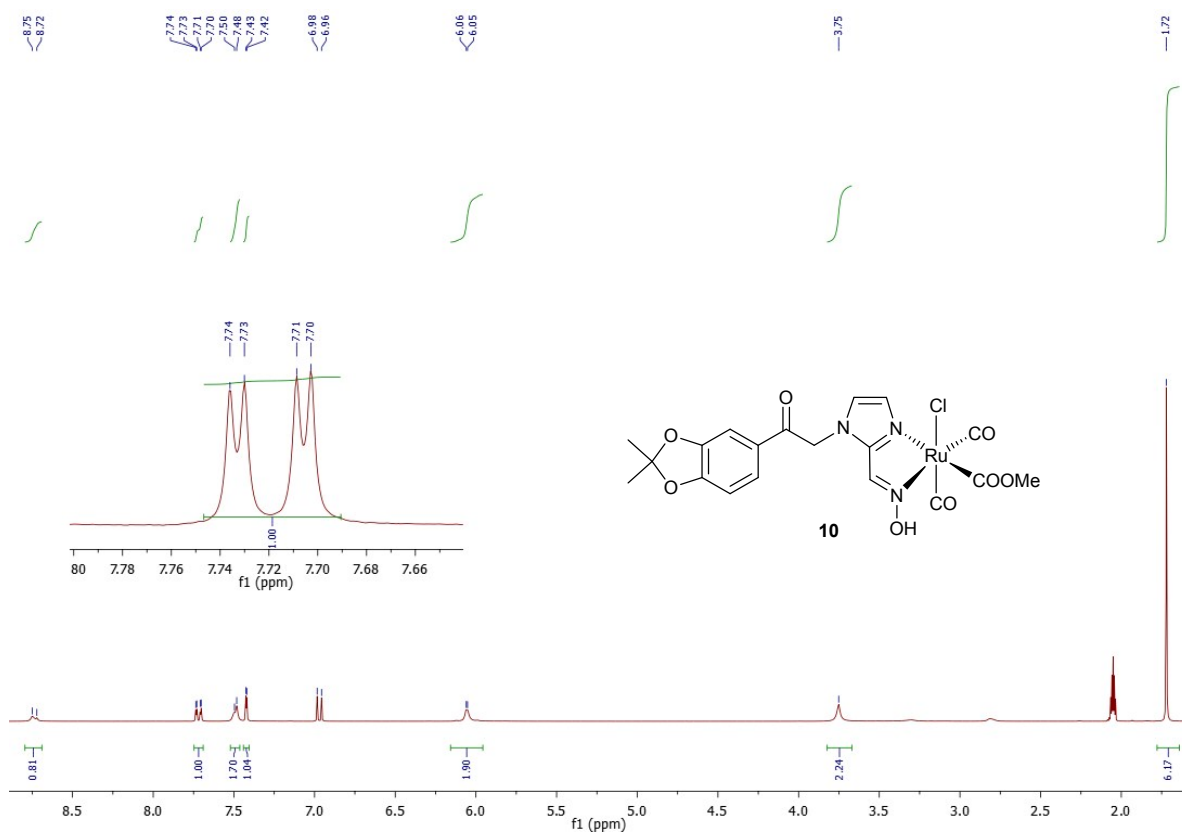


Fig. S1e ¹H NMR spectrum (300 MHz, DMSO-d₆) of (E)-1-(2-(2,2-dimethylbenzo[d][1,3]dioxol-5-yl)-2-oxoethyl)-1H-imidazol-2-carbaldehyde-oxime (**8**).





IR spectra

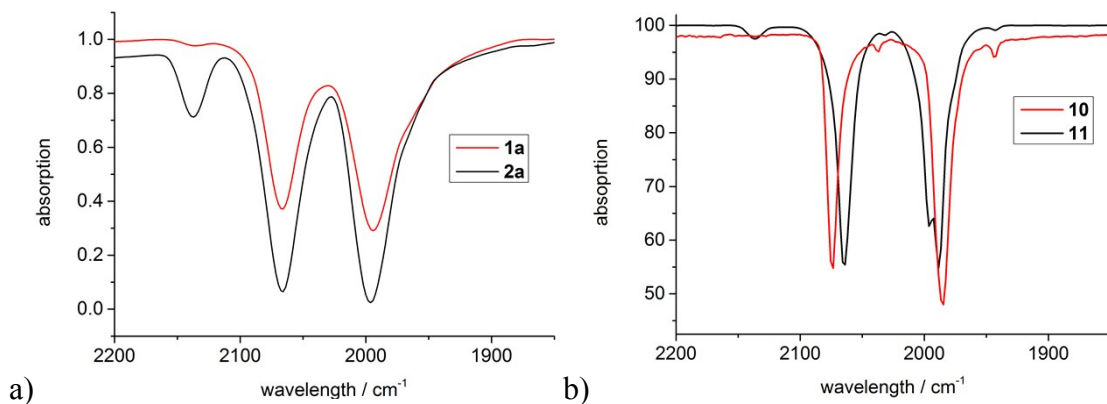


Fig. S2-1 Carbonyl region in IR spectra of compounds **1a** and **2a** (a) and the modified compounds **10** and **11** (b) in KBr disks. The bands at 2143 cm⁻¹ correspond to liberated free CO.

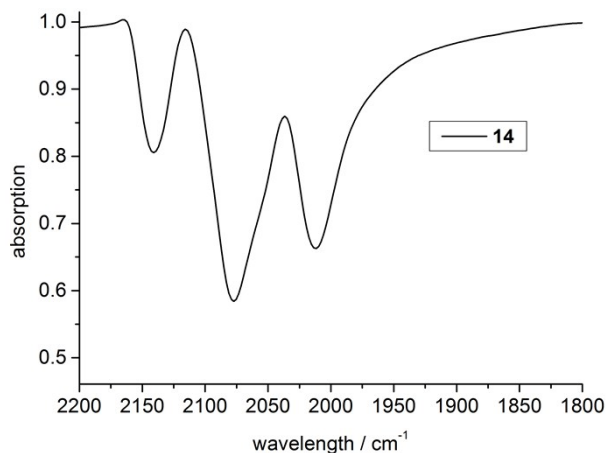


Fig. S2-2 IR spectrum of the oxime-based carbonyl **14** in KBr disks. The carbonyl region shows three strong absorptions at 2077 and 2012 cm⁻¹. The band at 2143 cm⁻¹ corresponds to liberated free CO.

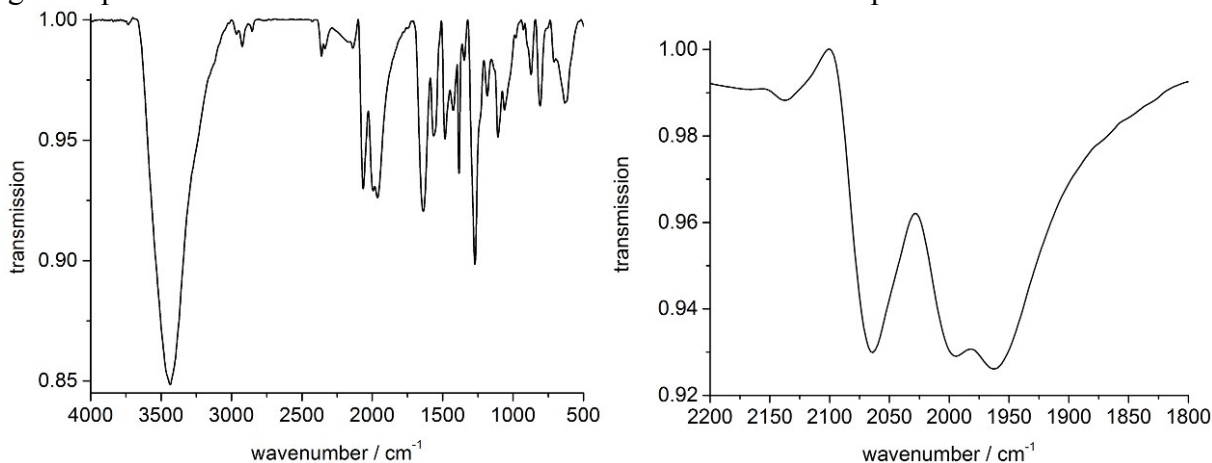


Fig. S2-3 IR spectra of the composite material **17** as KBr disk. The OH-vibration of the dextran is present at 3600-3000 cm⁻¹. The enlarged carbonyl region (right) shows three strong absorptions at 2064, 1995 and 1961 cm⁻¹.

Electron spray ionization mass spectra (ESI-MS)

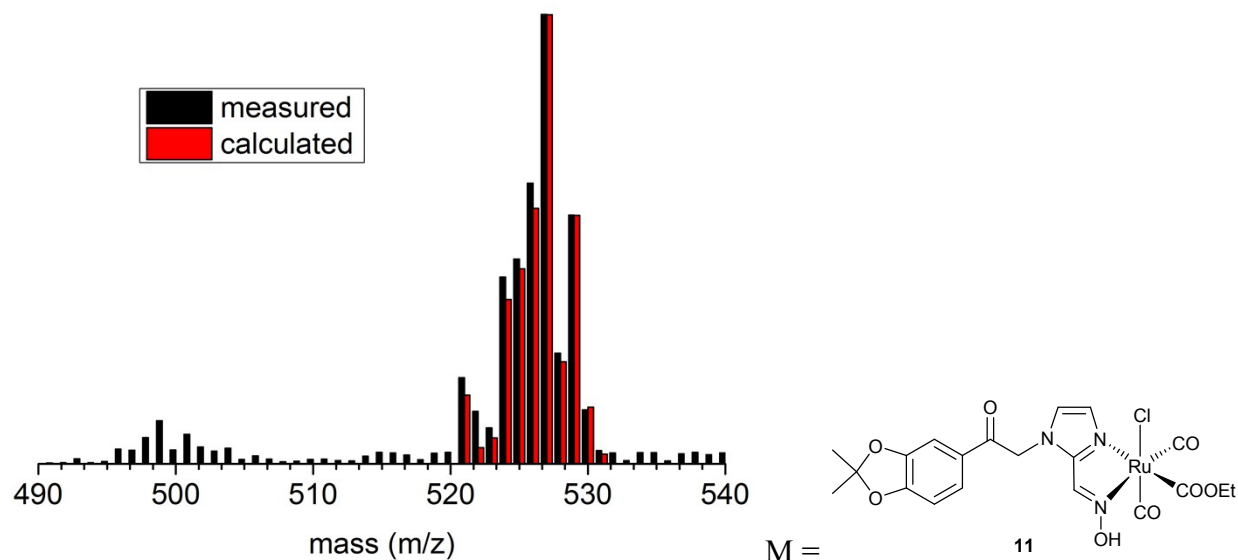


Fig. S3a Experimental (black) and calculated (red) electron spray ionization (ESI) mass spectrum of compound **11** in water/acetonitrile. $m/z = 527.0$ $[M - OEt^- - Cl^- - H^+ + CH_3CN]^+$, 499.1 $[M - CO/OEt^- - Cl^- - H^+ + CH_3CN]^+$.

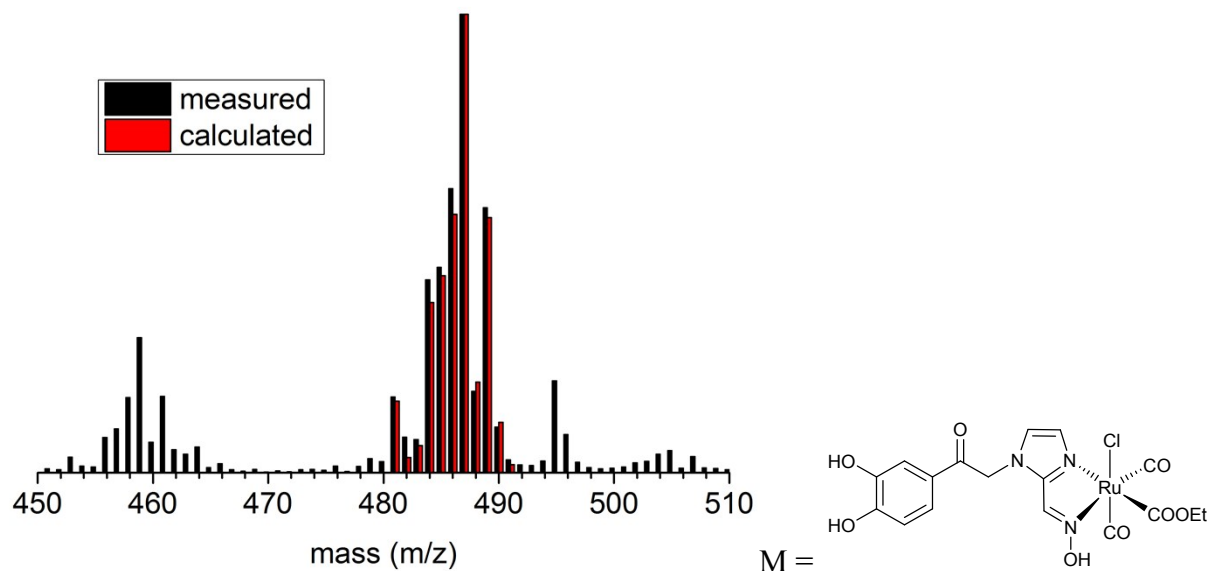


Fig. S3b Experimental (black) and calculated (red) electron spray ionization (ESI) mass spectrum of compound **14** in water/acetonitrile. $m/z = 487.0$ $[M - OEt^- - Cl^- - H^+ + CH_3CN]^+$, 459.2 $[M - CO/OEt^- - Cl^- - H^+ - CO + CH_3CN]^+$.

High-resolution electron spray ionization mass spectra (HR-ESI MS)

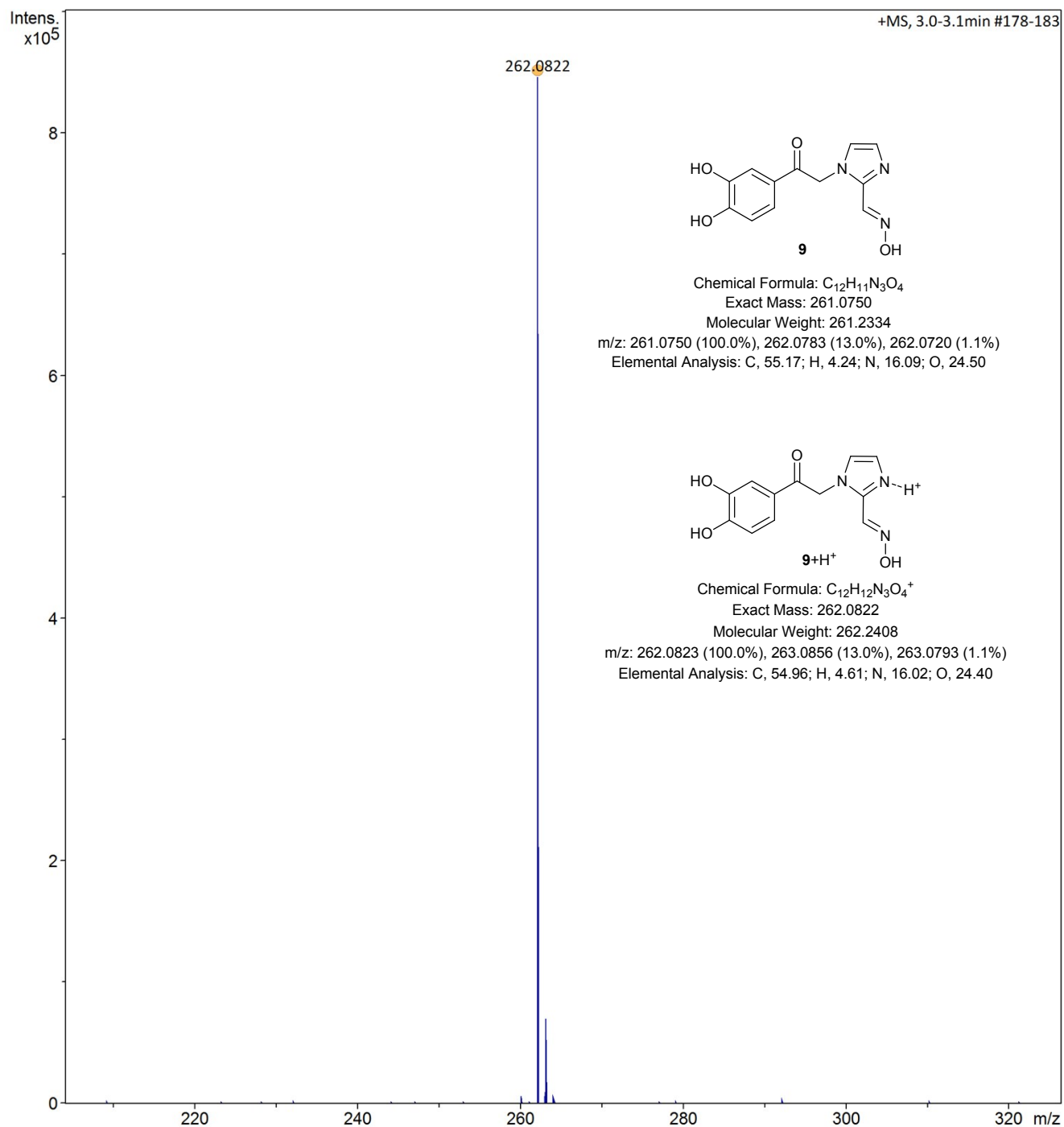


Fig. S4a Experimental electron spray ionization (ESI) mass spectrum of compound **9** in water/acetonitrile. $m/z = 262.0822$ fits very well to the calculated mass for the composition $[M + H]^+$ with $m/z = 262.8023$.

The absence of significant other peaks (besides the isotope pattern) confirms the purity of compound **9**.

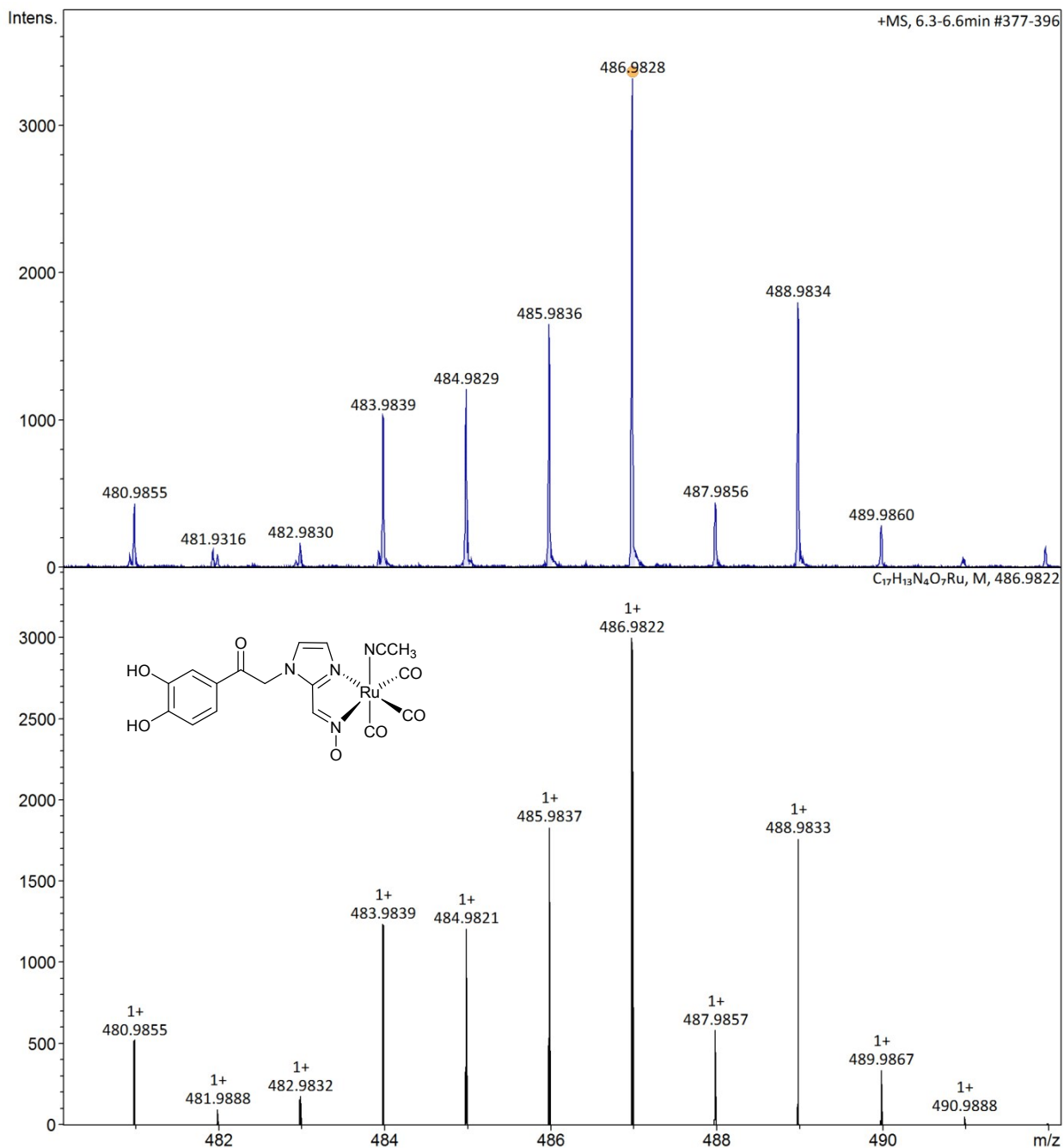


Fig. S4b HR-ESI MS with experimental (top-blue) and calculated (bottom) pattern around $m/z = 487$ of compound **14** in water/acetonitrile.

The experimental pattern at $m/z = 486.9828$ matches very well with the calculated pattern at $m/z = 486.9822$ for the composition $[M - OEt - Cl^- - H^+ + CH_3CN]^+$.

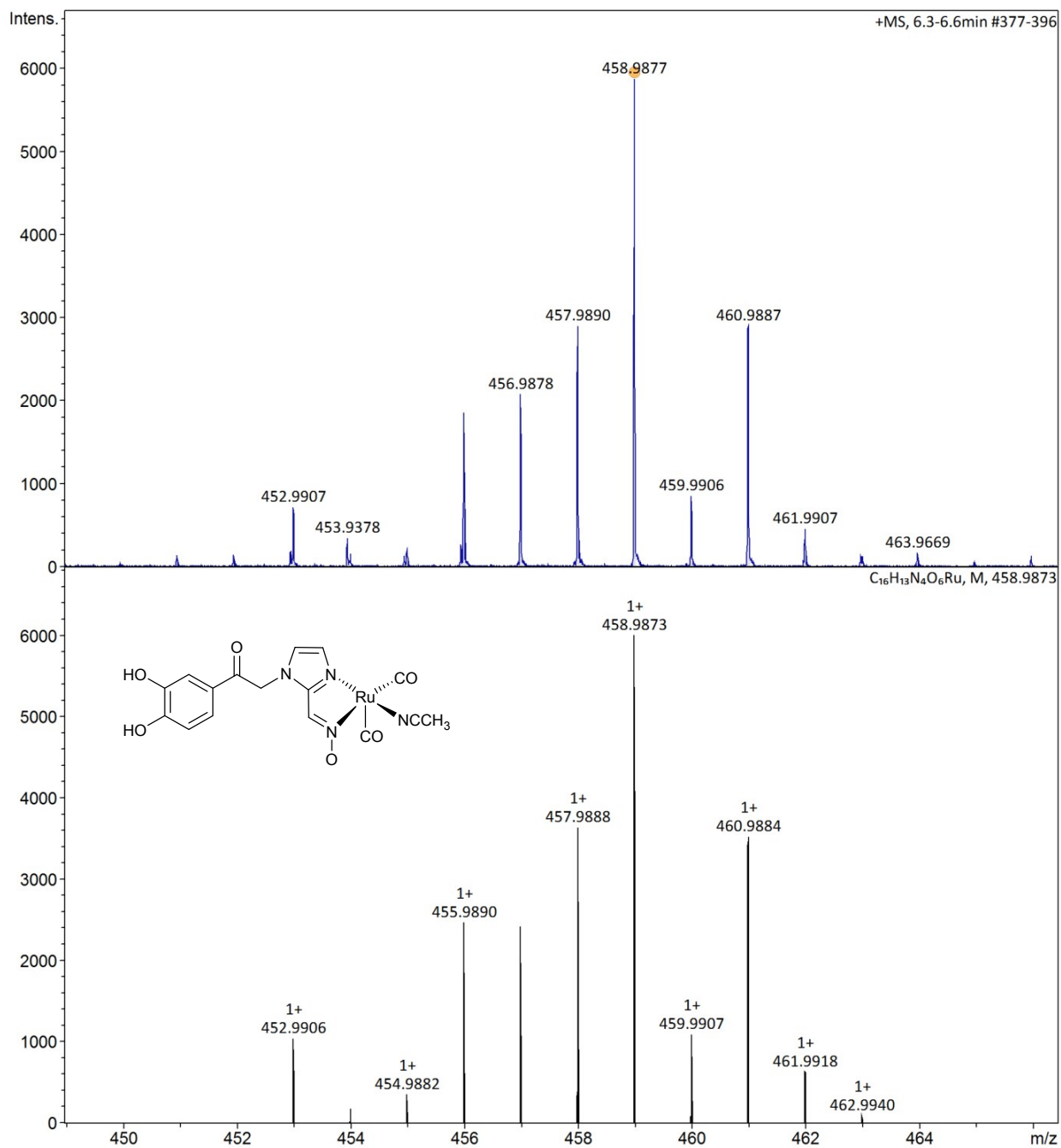


Fig. S4c HR-ESI MS with experimental (top-blue) and calculated (bottom) pattern around $m/z = 459$ of compound **14** in water/acetonitrile.

$m/z = 458.9877$ fits very well to the calculated mass for the composition $[M - CO/OEt - Cl - H + CH_3CN]^+$ with $m/z = 458.9873$.

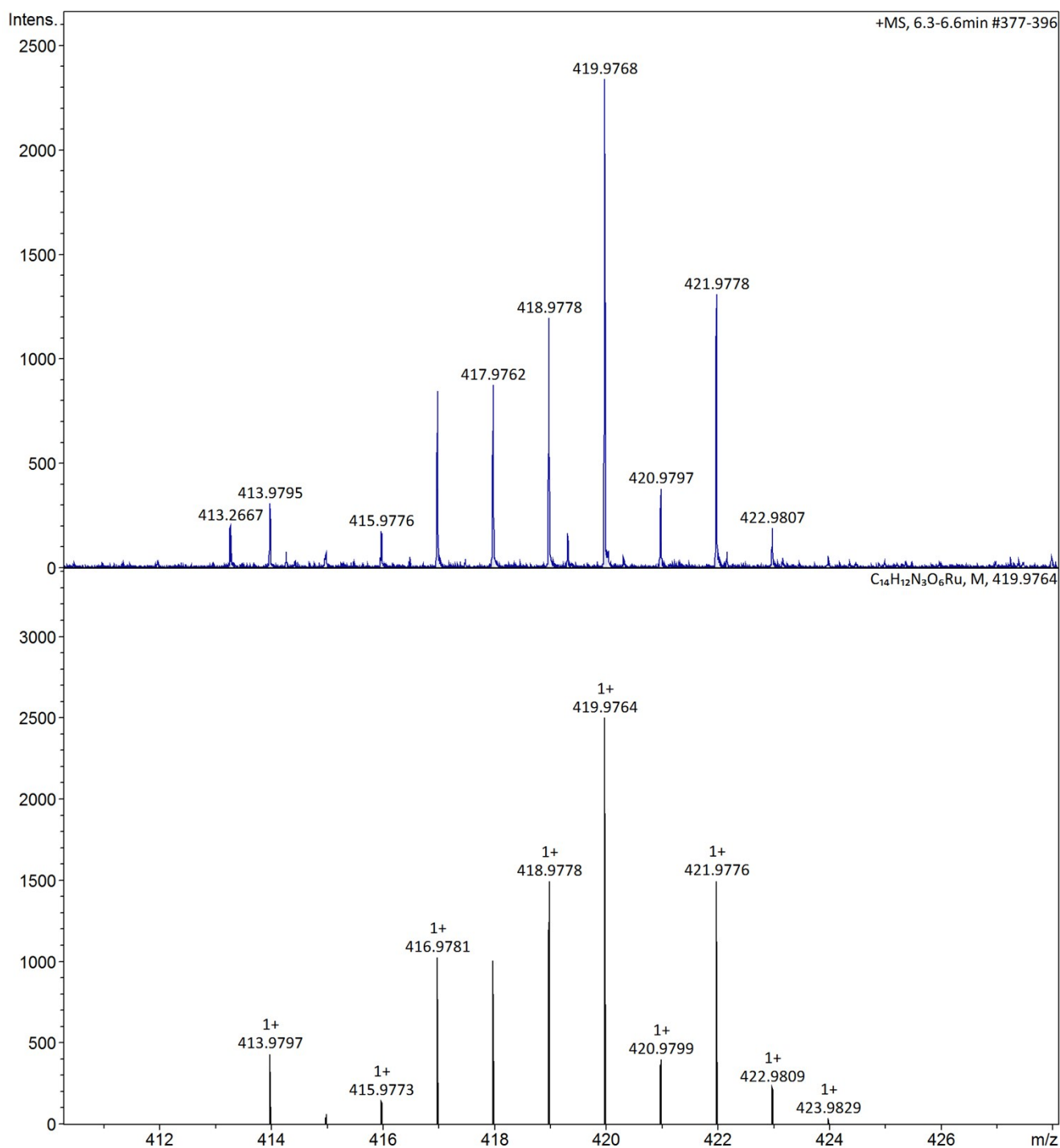


Fig. S4d HR-ESI MS with experimental (top-blue) and calculated (bottom) pattern around $m/z = 420$ of compound **14** in water/acetonitrile.

$m/z = 419.9768$ fits very well to the calculated mass for the composition $[M - CO/OEt^- - Cl^- + H]^+$ with $m/z = 419.9764$.

In a methanol (MeOH)/acetonitrile mixture the HR-ESI-MS spectra of **14** show an additional mass of $m/z = 477.9823$ $[M - OEt^- - Cl^- - CO + OMe^-]^+$ (calculated $m/z = 477.98244$) and $m/z = 449.9872$ $[M - OEt^- - Cl^- - CO + OMe^-]^+$ (calculated $m/z = 449.98752$).

CO release from compounds **1a** and **2a** in the myoglobin assay at various temperatures

The determination of the half-lives was performed by time-dependent visible absorption spectra and a plot of intensity changes at the wavelengths 541, 556 and 578 nm against time. By using an approximated exponential fit

$$y = y_o + Ae^{R_o x}$$

the half-life could be calculated for a first order kinetic with the following formula:

$$t_{1/2} = \ln 2 / -R_o$$

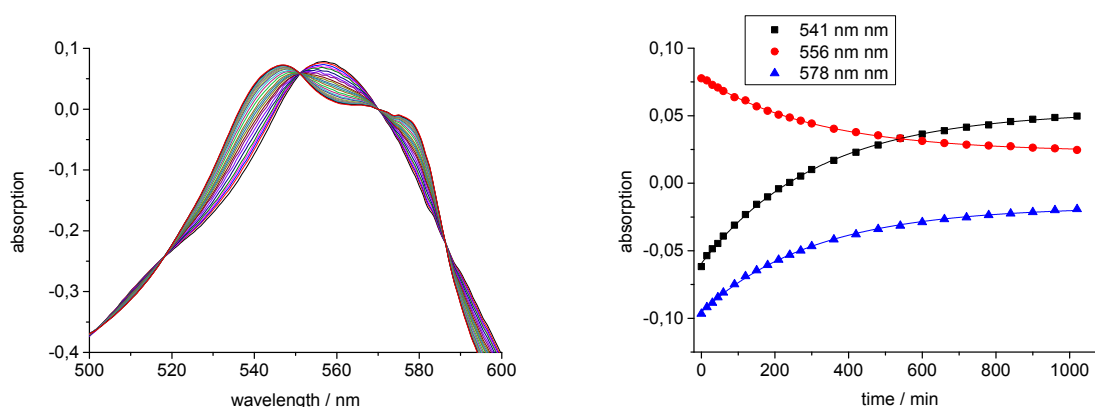


Fig. S5: Time-dependent visible absorption spectra (left) and plot of the intensity changes of selected wavelengths (right) of Ru(imidazole-2-carbaldehyde-oxime)(methoxycarbonyl)(CO)₂Cl (**1a**) with myoglobin assay at 20 °C to yield an averaged half-life for **1a** of $t_{1/2} = 220 \pm 23$ min.

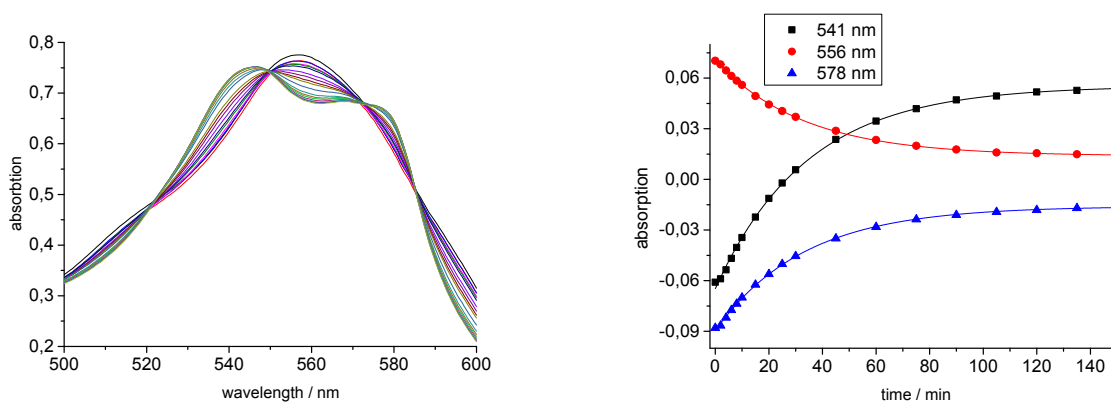


Fig. S6: Time-dependent visible absorption spectra (left) and plot of the intensity changes of selected wavelengths (right) of Ru(imidazole-2-carbaldehyde-oxime)(methoxycarbonyl)(CO)₂Cl (**1a**) with myoglobin assay at 37 °C to yield an averaged half-life for **1a** of $t_{1/2} = 21 \pm 2$ min.

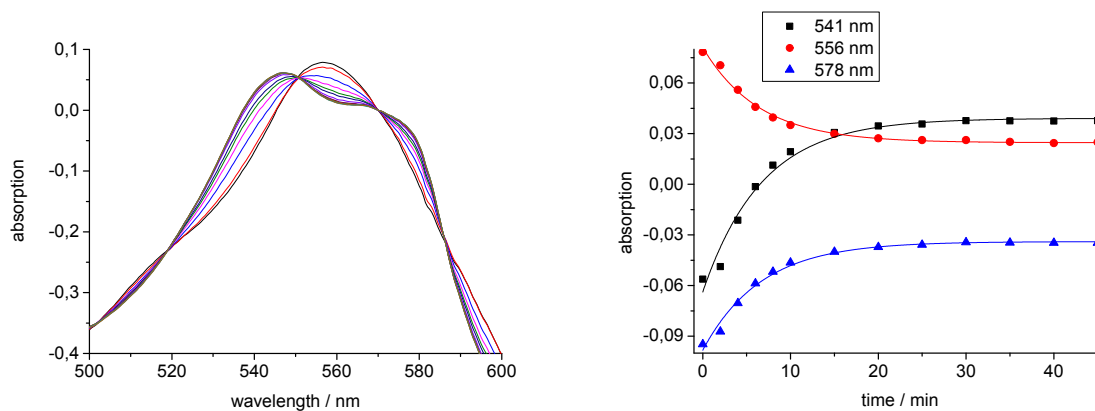


Fig. S7: Time-dependent visible absorption spectra (left) and plot of the intensity changes of selected wavelengths (right) of Ru(imidazole-2-carbaldehyde-oxime)(methoxycarbonyl)(CO)₂Cl (**1a**) with myoglobin assay at 50 °C to yield an averaged half-life for **1a** of $t_{1/2} = 5 \pm 1$ min.

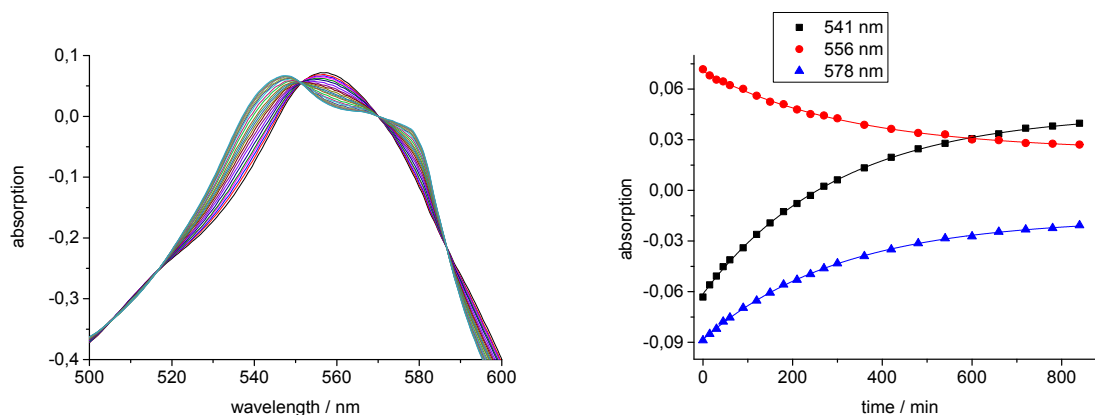


Fig. S8: Time-dependent visible absorption spectra (left) and plot of the intensity changes of selected wavelengths (right) of Ru(imidazole-2-carbaldehyde-oxime)(ethoxycarbonyl)(CO)₂Cl (**2a**) with myoglobin assay at 20 °C to yield an averaged half-life for **2a** of $t_{1/2} = 226 \pm 9$ min.

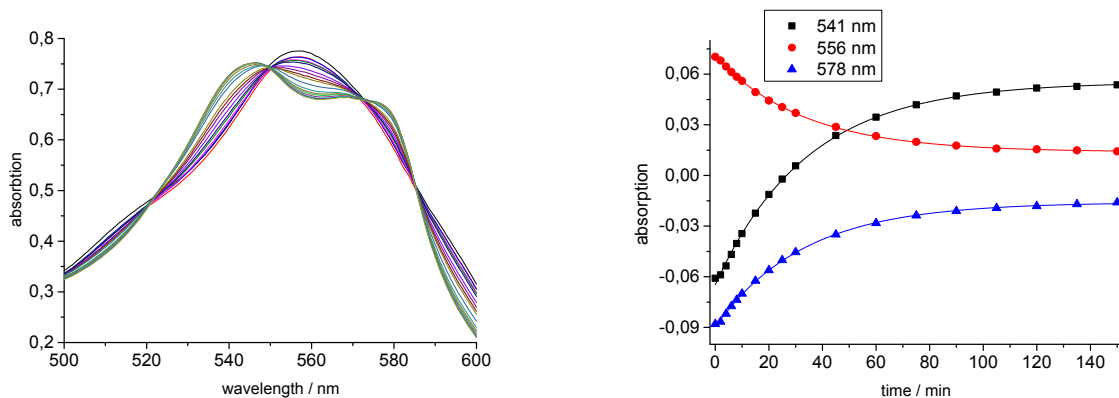


Fig. S9: Time-dependent visible absorption spectra (left) and plot of the intensity changes of selected wavelengths (right) of Ru(imidazole-2-carbaldehyde-oxime)(ethoxycarbonyl)(CO)₂Cl (**2a**) with myoglobin assay at 37 °C to yield an averaged half-life for **2a** of $t_{1/2} = 15 \pm 1$ min.

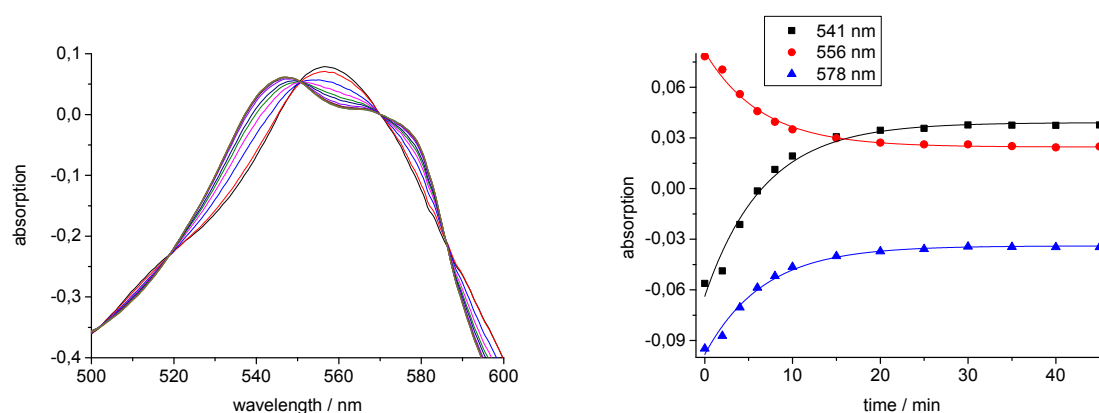


Fig. S10: Time-dependent visible absorption spectra (left) and plot of the intensity changes of selected wavelengths (right) of Ru(imidazole-2-carbaldehyde-oxime)(ethoxycarbonyl)(CO)₂Cl (**2a**) with myoglobin assay at 50 °C to yield an averaged half-life for **2a** of $t_{1/2} = 6 \pm 1$ min.

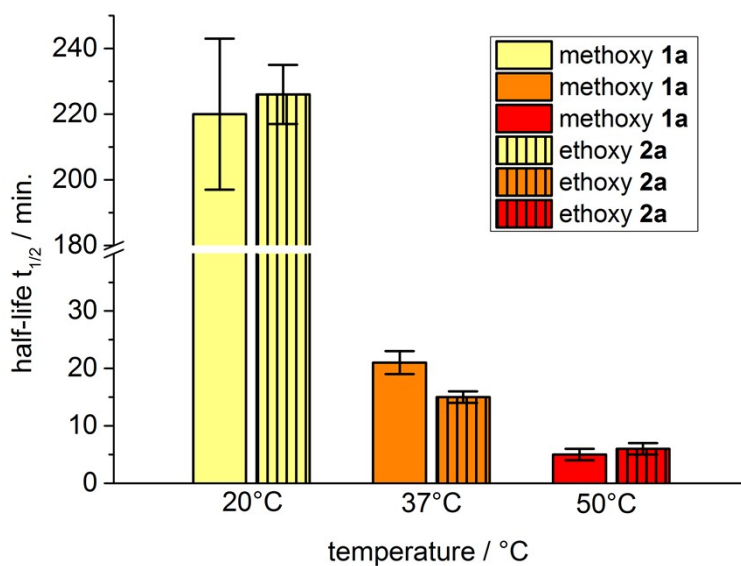


Fig. S11: Bar diagram for the half-lives from Ru(imidazole-2-carbaldehyde-oxime)-(methoxycarbonyl)(CO)₂Cl (**1a**, left bars) and Ru(imidazole-2-carbaldehyde-oxime)(ethoxycarbonyl)(CO)₂Cl (**2a**, right bars) at 20 °C, 37 °C and 50 °C (with standard deviations) in the myoglobin assay.

CO release from compounds **10** and **11** in the myoglobin assay at various temperatures

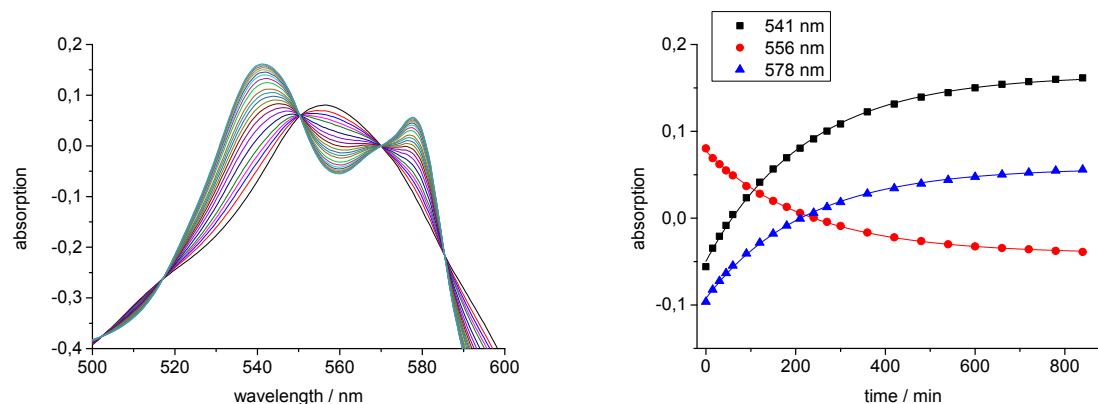


Fig. S12: Time-dependent visible absorption spectra (left) and plot of the intensity changes of selected wavelengths (right) of Ru(η²-**8**)(methoxycarbonyl)(CO)₂Cl (**10**) with myoglobin assay at 20 °C to yield an averaged half-life for **10** of $t_{1/2} = 172 \pm 23$ min.

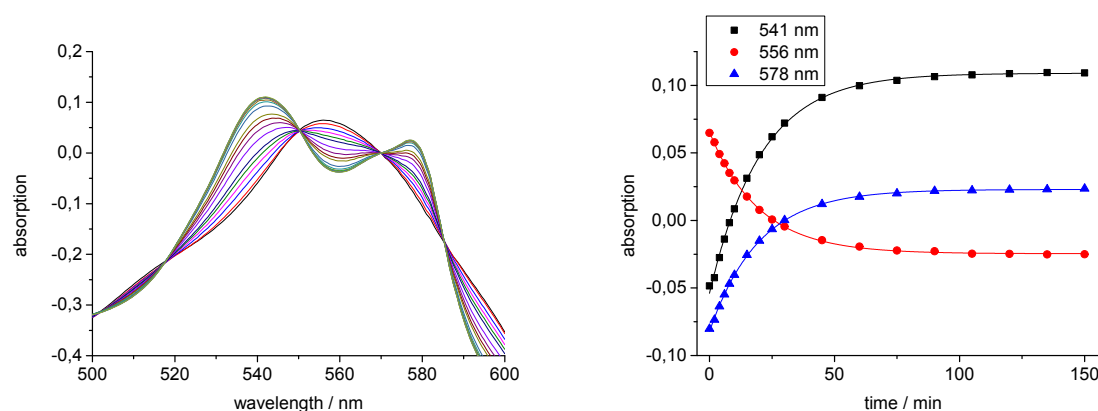


Fig. S13: Time-dependent visible absorption spectra (left) and plot of the intensity changes of selected wavelengths (right) of Ru(η²-**8**)(methoxycarbonyl)(CO)₂Cl (**10**) with myoglobin assay at 37 °C to yield an averaged half-life for **10** of $t_{1/2} = 18 \pm 1$ min.

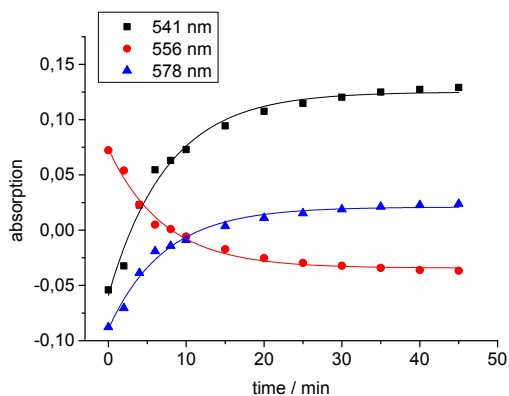
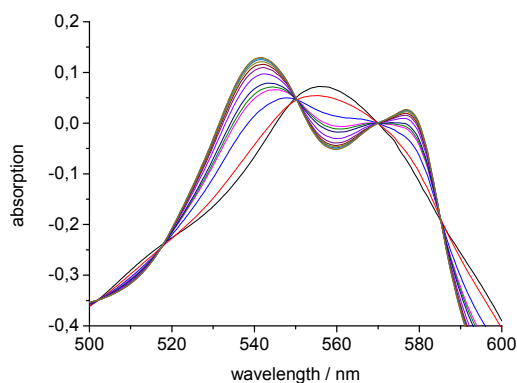


Fig. S14: Time-dependent visible absorption spectra (left) and plot of the intensity changes of selected wavelengths (right) of Ru(η^2 -**8**)(methoxycarbonyl)(CO)₂Cl (**10**) with myoglobin assay at 50 °C to yield an averaged half-life for **10** of $t_{1/2} = 4 \pm 1$ min.

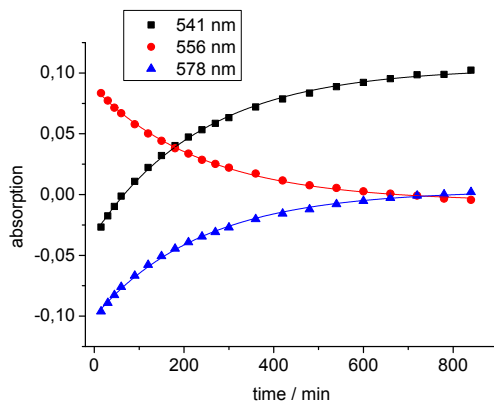
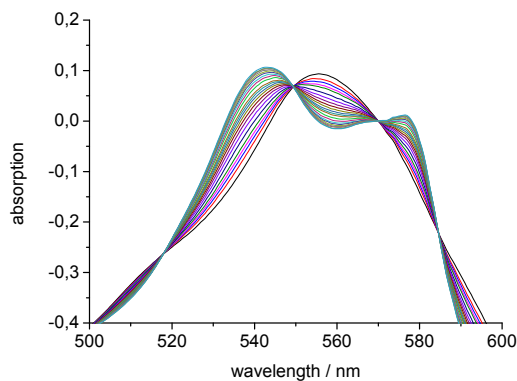


Fig. S15: Time-dependent visible absorption spectra (left) and plot of the intensity changes of selected wavelengths (right) of Ru(η^2 -**8**)(ethoxycarbonyl)(CO)₂Cl (**11**) with myoglobin assay at 20 °C to yield an averaged half-life for **11** of $t_{1/2} = 155 \pm 13$ min.

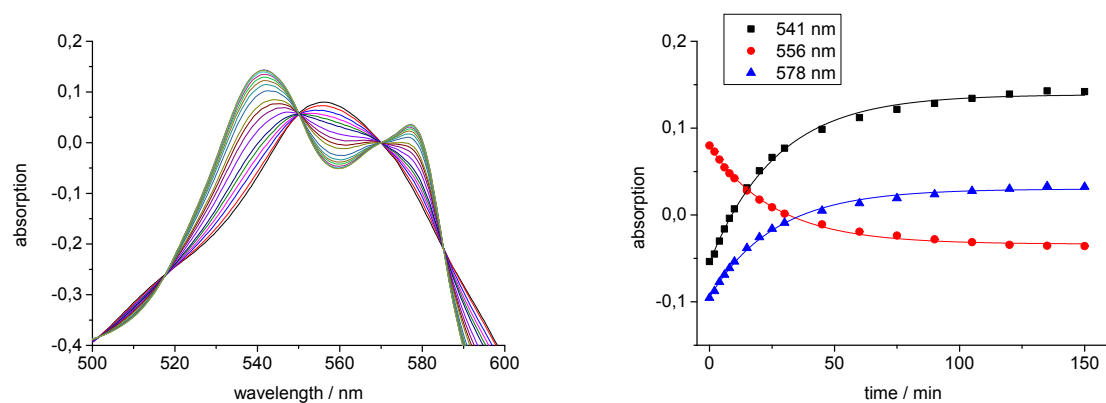


Fig. S16: Time-dependent visible absorption spectra (left) and plot of the intensity changes of selected wavelengths (right) of Ru(η^2 -**8**)(ethoxycarbonyl)(CO)₂Cl (**11**) with myoglobin assay at 37 °C to yield an averaged half-life for **11** of $t_{1/2} = 18 \pm 1$ min.

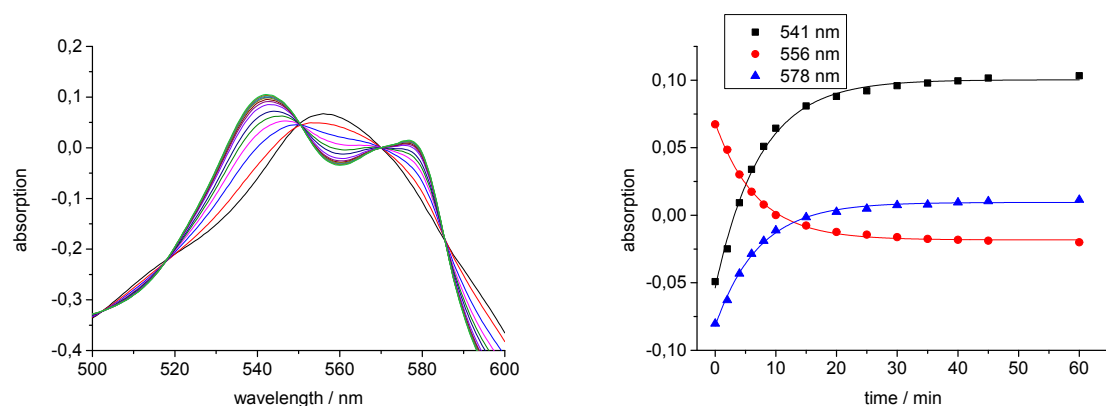


Fig. S17: Time-dependent visible absorption spectra (left) and plot of the intensity changes of selected wavelengths (right) of Ru(η^2 -**8**)(ethoxycarbonyl)(CO)₂Cl (**11**) with myoglobin assay at 50 °C to yield an averaged half-life for **11** of $t_{1/2} = 4 \pm 1$ min.

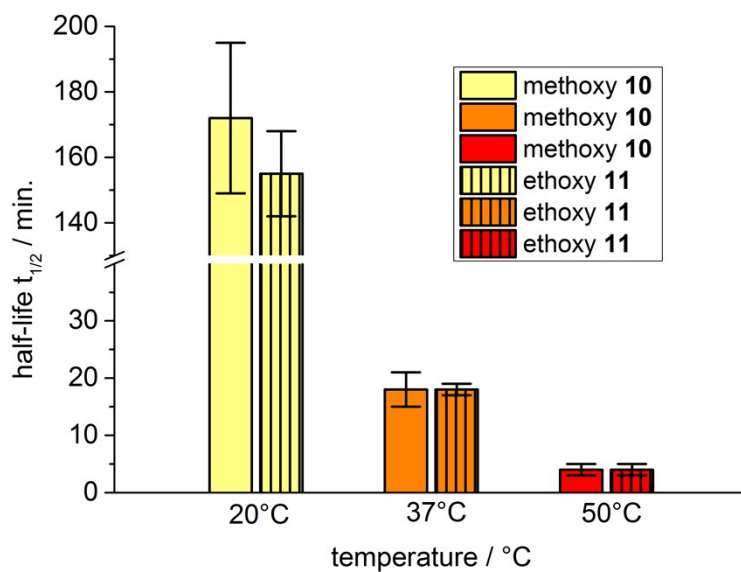


Fig. S18: Bar diagram for the half-lives from $\text{Ru}(\eta^2\text{-8})(\text{COOMe})(\text{CO})_2\text{Cl}$ (**10**) and $\text{Ru}(\eta^2\text{-8})(\text{ethoxycarbonyl})(\text{CO})_2\text{Cl}$ (**11**) at 20 °C, 37 °C and 50 °C (with standard deviations) in the myoglobin assay.

CO release from compound **14** in the myoglobin assay at various temperatures

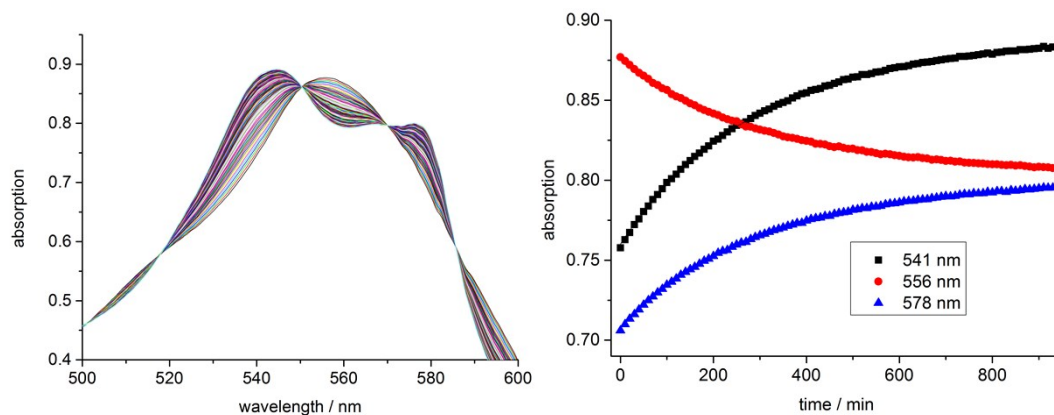


Fig. S19: Time-dependent visible absorption spectra (left) and plot of the intensity changes of selected wavelengths (right) of Ru(η^2 -**9**)(ethoxycarbonyl)(CO)₂Cl (**14**) with myoglobin assay at 20 °C to yield an averaged half-life for **14** of $t_{1/2} = 207 \pm 6$ min. (Spectra were collected every 10 min.)

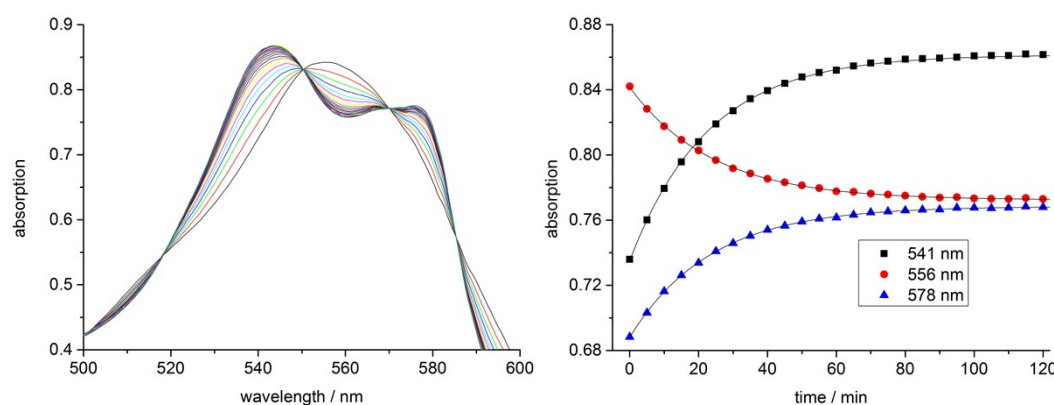


Fig. S20: Time-dependent visible absorption spectra (left) and plot of the intensity changes of selected wavelengths (right) of Ru(η^2 -**9**)(ethoxycarbonyl)(CO)₂Cl (**14**) with myoglobin assay at 37 °C to yield an averaged half-life for **14** of $t_{1/2} = 16 \pm 1$ min.

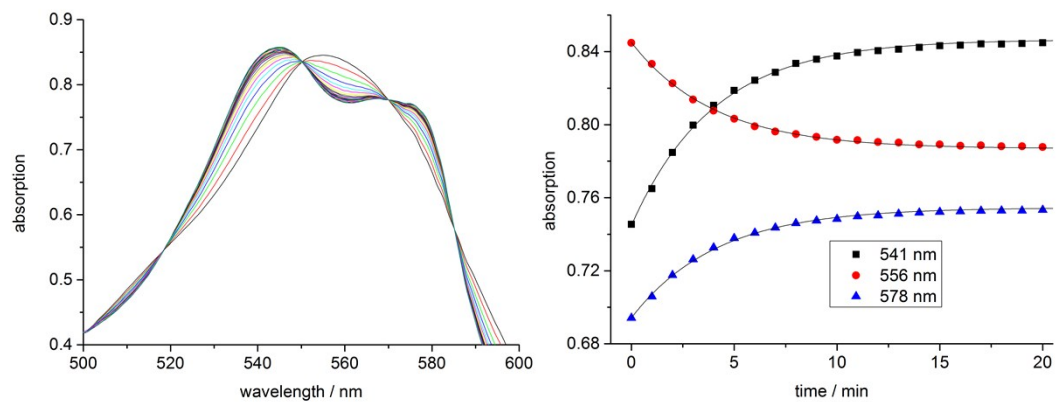


Fig. S21: Time-dependent visible absorption spectra (left) and plot of the intensity changes of selected wavelengths (right) of Ru(η^2 -**9**)(ethoxycarbonyl)(CO)₂Cl (**14**) with myoglobin assay at 50 °C to yield an averaged half-life for **14** of $t_{1/2} = 3 \pm 1$ min.

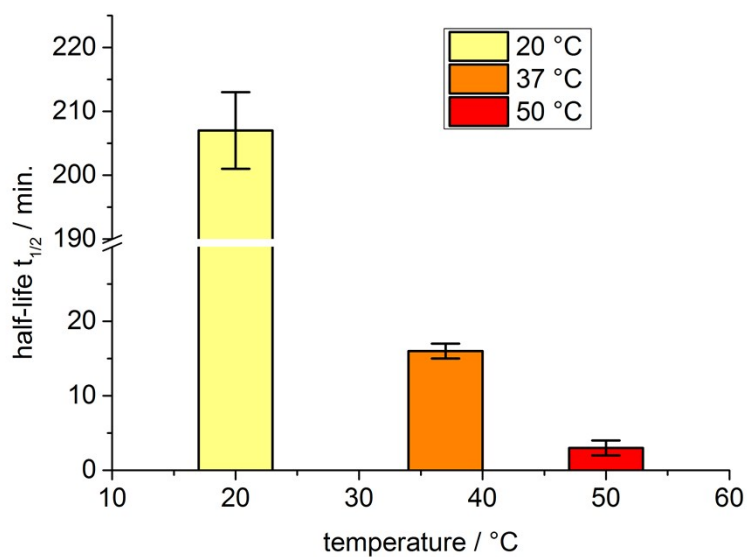


Fig. S22: Half-lives from Ru(η^2 -**9**)(ethoxycarbonyl)(CO)₂Cl (**14**) at 20 °C, 37 °C and 50 °C (with standard deviations) in the myoglobin assay.

CO release from the composite material alginate@dextran@oximeCORM@IONP (18) in the myoglobin assay at various temperatures

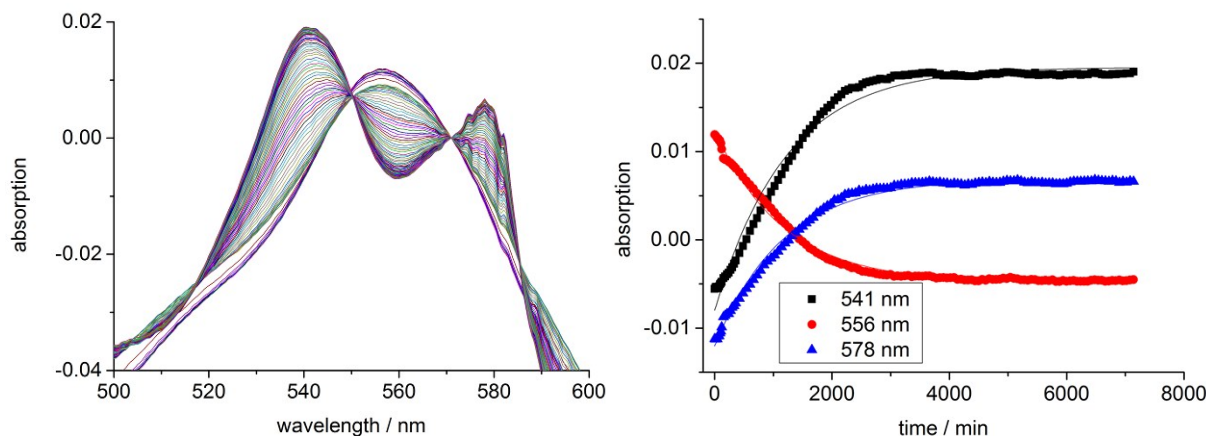


Fig. S23: Time-dependent visible absorption spectra (left) and plot of the intensity changes of selected wavelengths (right) of alginate@dextran@oximeCORM@IONP (**18**) with myoglobin assay at 20 °C to yield an averaged half-life for **18** of $t_{1/2} = 814 \pm 23$ min. (Spectra were collected every 10 min.)

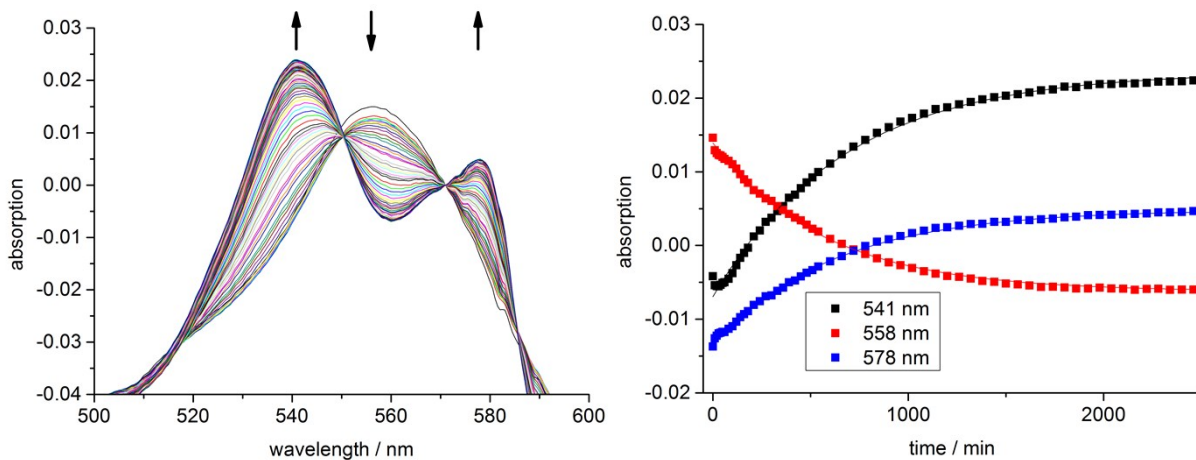


Fig. S24: Time-dependent visible absorption spectra (left) and plot of the intensity changes of selected wavelengths (right) of alginate@dextran@oximeCORM@IONP (**18**) with myoglobin assay at 37 °C to yield an averaged half-life for **18** of $t_{1/2} = 346 \pm 83$ min.

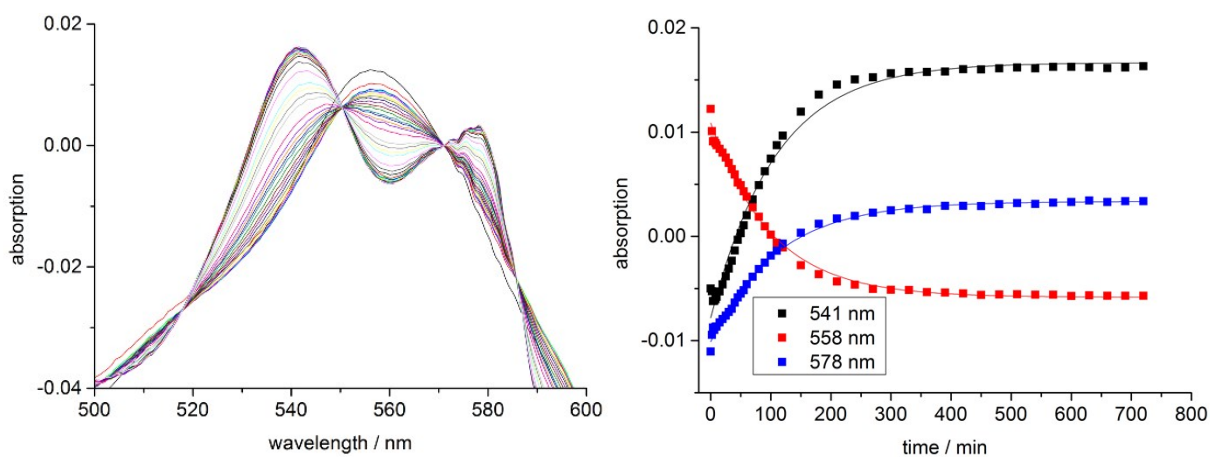


Fig. S25: Time-dependent visible absorption spectra (left) and plot of the intensity changes of selected wavelengths (right) of alginate@dextran@oximeCORM@IONP (**18**) with myoglobin assay at 50 °C to yield an averaged half-life for **18** of $t_{1/2} = 73 \pm 1$ min.



Fig. S26: Picture of the alginate spheres on the bottom of a temperature controllable UV/VIS cell with myoglobin solution.

CO release from compound **18** with applied alternating (AC) magnetic field

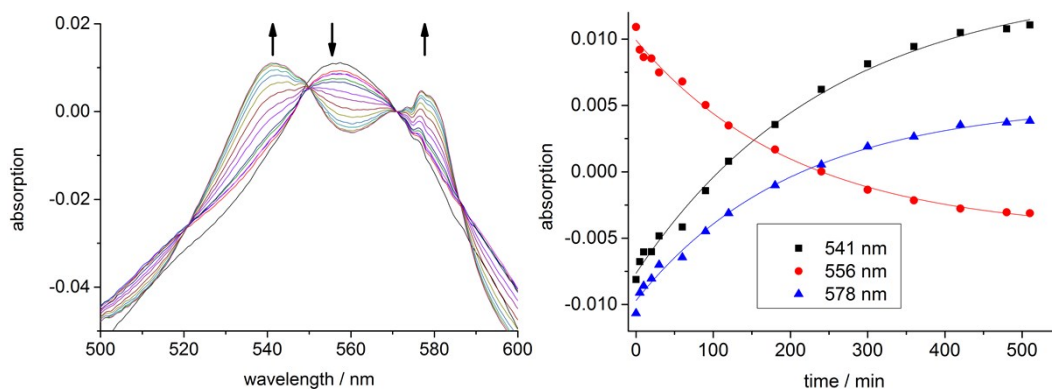


Fig. S27: Time-dependent visible absorption spectra (left) and plot of the intensity changes of selected wavelengths (right) of alginate@dextran@oximeCORM@IONP (**18**) with myoglobin assay at 37 °C with the applied alternating (AC) magnetic field (31.7 kAm⁻¹, 247 kHz, 39.9 mTesla) to yield an averaged half-life for **18** of $t_{1/2} = 153 \pm 27$ min.

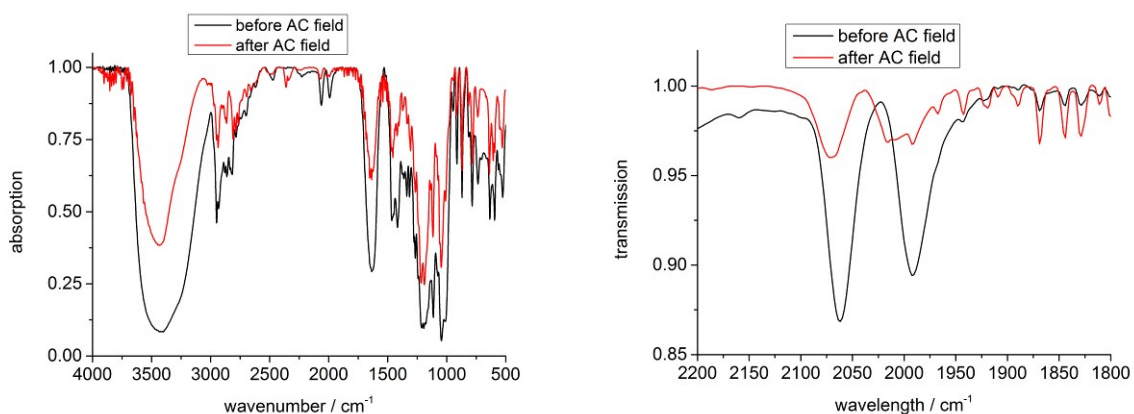


Fig. S28: IR spectra of the composite material alginate@dextran@oximeCORM@IONP (**18**) in KBr disks before and after the CO release in the alternating (AC) magnetic field. The carbonyl region (enlarged at right) showed two strong absorptions at 2061, 1991 cm⁻¹ before the CO release (black) and absorptions shifted to 2071, 2015 and 1992 cm⁻¹ (red) after the CO release.

Determined amount of released CO

We calculated the amount of released CO with equation (1):

$$c(\text{MyoCO}) = \left(\frac{A(t)}{l} - \frac{A(t=0)}{l} \right) \cdot \frac{1}{\varepsilon_{540\text{ nm}}(\text{MyoCO}) - A(t=0) / c_0(\text{Myo}) \cdot l} \quad \text{Eq. (1)}$$

with $A(t)$ = absorption at time t ,

$A(t=0)$ = absorption at time $t=0$,

l = path length of the cuvette,

$\varepsilon_{540\text{ nm}}(\text{MyoCO}) = 15.4 \text{ L} \cdot \text{mmol}^{-1} \cdot \text{cm}^{-1}$, and $c_0(\text{Myo})$ = concentration of myoglobin from first absorption spectrum (here volume of cuvette $V = 0.0014 \text{ L}$).

The correction of the spectra was done by the method of ATKIN *et al.*³ The amount of CO was determined with the Lambert-Beer-law. The results are shown in Table S1.

Table S1 Amount of carbon monoxide released from the compounds **10**, **11** and **14** in mol carbon monoxide per mol Ru.

compound	mol carbon monoxide per mol Ru
10	0.9(1)
11	0.8(1)
14	0.9(1)
18	0.2(1)

It is now known and quantified from recent literature that CORM-2 will lose 1.8 CO as CO₂ in water within 24 h.⁴

Leaching experiments

Three time-dependent leaching experiments were prepared by dispersing 20 mg each of dextran@oximeCORM@IONP (**17**) in 1 mL MOPS buffer (pH 7.4) and mixing this solution with 2.4 mL alginate solution according to the synthetic procedure of alginate@dextran@oximeCORM@IONP (**18**). After the formation of the alginate spheres with calcium chloride solution and fully crosslinking of the alginate network, all of the formed spheres were washed as described. Two samples were stored in 5 mL MOPS buffer (pH 7.4) for 12 h and 24 h and washed twice with 5 mL deionized water afterwards. The ruthenium quantity in the alginate composite directly after the preparation of **18** (t_0)

and after the storage in buffered solution for 12 h (t_{12h}) and 24 h (t_{24h}), was determined by AAS and yielded in: $t_0 = 0.60\text{wt}\%$, $t_{12h} = 0.17\text{wt}\%$ and $t_{24h} = 0.13\text{wt}\%$ in the 20 mg sample of dextran@oximeCORM@IONP (**17**). This corresponds to a leaching of 72% after 12 h and 78% after 24 h of the initial amount of ruthenium into the surrounding solution. These results suggest a weaker ruthenium metal-oxime bond than the metal-amino-alkoxide bond in CORM-3 analogous system which we described earlier.⁵

Dynamic light scattering, DLS and transmission electron microscopy, TEM measurements of functionalized maghemite nanoparticles

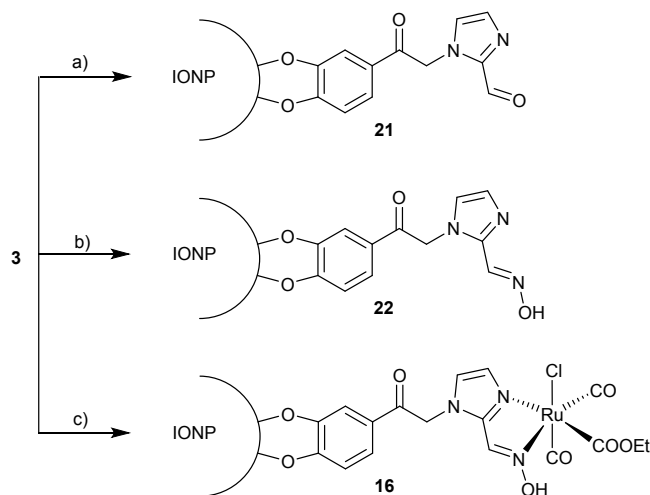


Fig. S29: Synthesis of functionalized maghemite nanoparticles with the ligands **9**, **11** and **15**. a) d.d. water, NaOH (pH = 10), **9**; b) d.d. water, NaOH (pH = 10), **11**; a) d.d. water, NaOH (pH = 10), **15**.

Immobilization of 1-(2-(3,4-dihydroxyphenyl)-2-oxoethyl)-1H-imidazole-2-carbaldehyde (5) on maghemite nanoparticles (21): A suspension of 100 mg of **5** in 6 mL of d.d. water was mixed with sodium hydroxide solution until pH = 10 was reached. Maghemite nanoparticles (**3**) were added (2 mL, 10 mg/mL) and the solution was stirred for 15 min. After neutralizing with hydrochloric acid the solution was combined with 100 mL acetone and the formed solid separated with centrifugation. The solid was washed with 3x 5mL of acetone and dried under vacuum. Yield: 25 mg, IR (KBr): $\tilde{\nu} = 1686, 1488 \text{ cm}^{-1}$.

Immobilization of 1-(2-(3,4-dihydroxyphenyl)-2-oxoethyl)-1H-imidazol-2-carbaldehyde-oxime (9) on maghemite nanoparticles (22): A suspension of 5 mg of **9** in 2 mL of d.d. water was mixed with a few drops of 0.1 mol/L sodium hydroxide solution to form a clear solution. Maghemite nanoparticles (**3**) were added (1 mL, 10 mg/mL) and the solution was stirred for 15 min. After neutralizing with hydrochloric acid the solution was combined with 50 mL of acetone and the formed solid separated by centrifugation. The solid was washed with 3x 5mL of acetone and dried under vacuum. Yield: 7 mg, IR (KBr): $\tilde{\nu} = 1638, 1490 \text{ cm}^{-1}$.

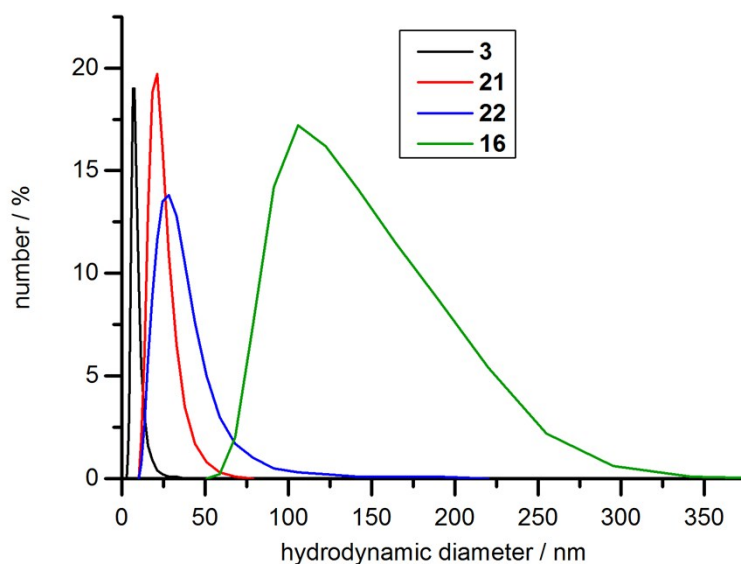


Fig. S30: Size distribution of the hydrodynamic diameter of particles of **3** (black), **21** (red), **22** (blue) and **16** (green) in water ($c = 1 \text{ mg/mL}$) from dynamic light scattering (DLS) investigations. The broad distribution of **16** (green) is due to sedimentation processes during the measurement. See Table S2 for the diameter values.

Table S2: Average hydrodynamic diameters of functionalized maghemite nanoparticles.

compound	medium hydrodynamic diameter [nm] ^a
maghemite (IONP, 3)	8 ± 2
maghemite + aldehyde (21)	23 ± 4
maghemite + oxime (22)	32 ± 10
maghemite + CORM (23) ^b	133 ± 31

^a Measured as aqueous dispersions with a minimum concentration of 1 mg/mL in doubly deionized water. With standard deviation σ in nm.

^b The large hydrodynamic diameter is due to low water solubility of the maghemite+CORM nanoparticles so that larger sedimentated aggregates exist in the dispersion; cf. Fig. S34.

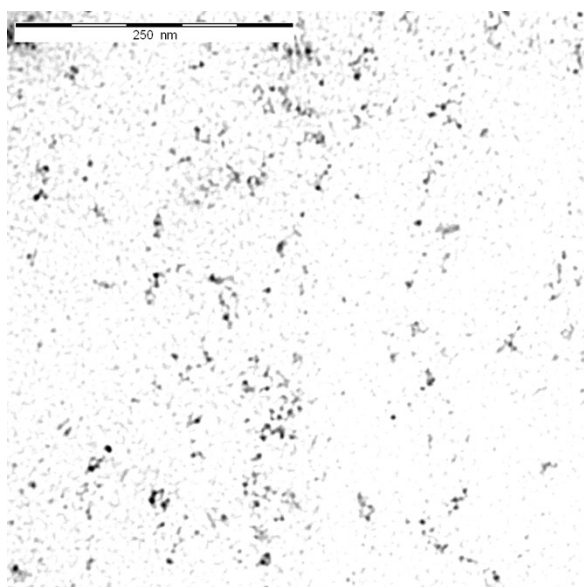


Fig. S31: TEM image of maghemite nanoparticles (3)

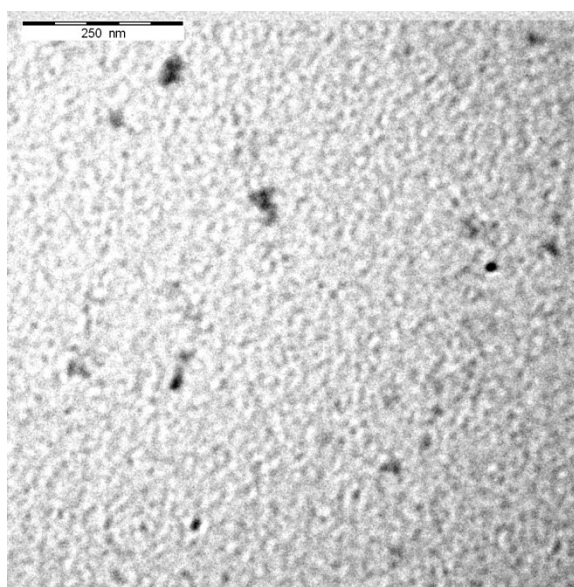


Fig. S32: TEM image of the aldehyde-functionalized maghemite nanoparticles 21.

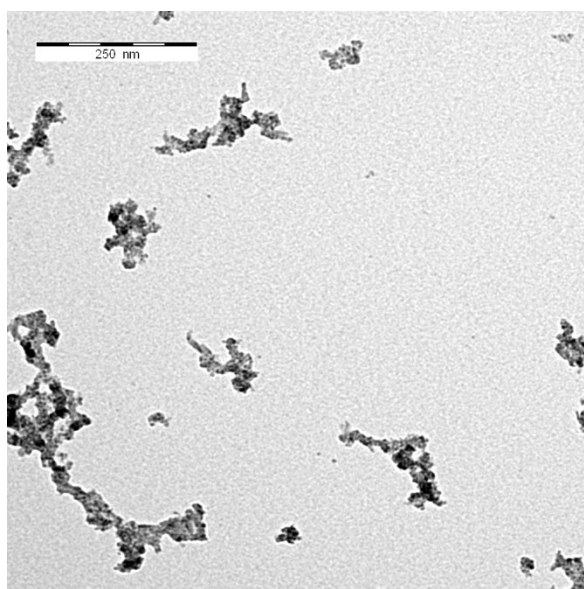


Fig. S33: TEM image of the oxime-functionalized maghemite nanoparticles 22.

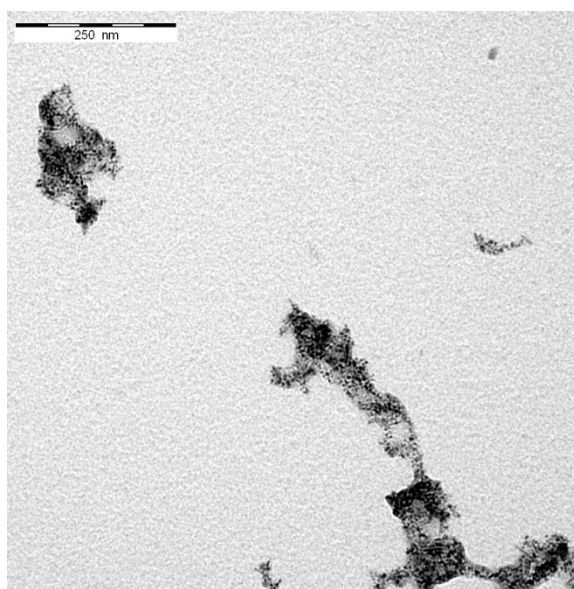


Fig. S34: TEM image of the CORM-functionalized nanoparticles 16.

Toxicity Tests

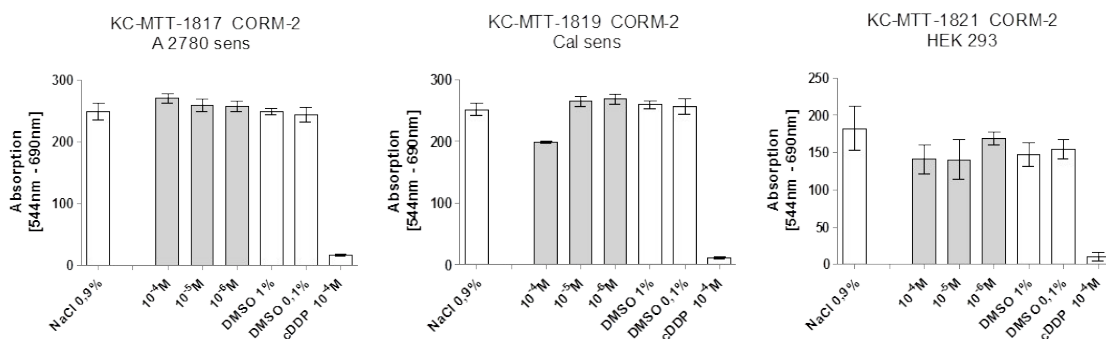


Fig. S35: Toxicity test of CORM-2 in different concentrations, sodium chloride (0.9%), DMSO (1% and 0.1% as solvent), and cDDP (10^{-4} mol/L Cisplatin) with the cells A2780 (left), CalSens (middle) and HEK293 (right).

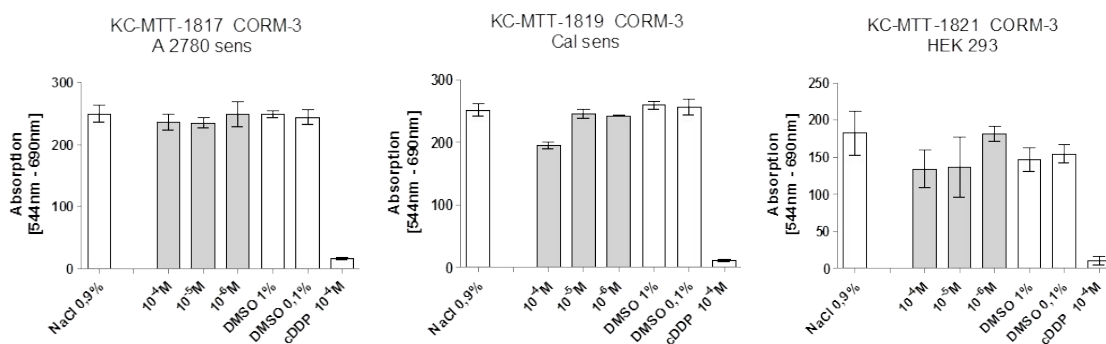


Fig. S36: Toxicity test of CORM-3 in different concentrations, sodium chloride (0.9%), DMSO (1% and 0.1% as solvent), and cDDP (10^{-4} mol/L Cisplatin) with the cells A2780 (left), CalSens (middle) and HEK293 (right).

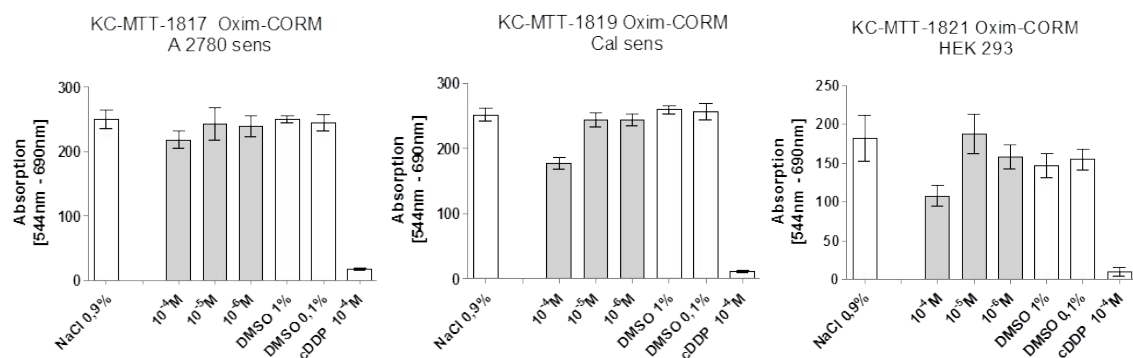


Fig. S37: Toxicity test of Ru(η^2 -9)(COOEt)(CO)₂Cl (**14**) (here labeled Oxim-CORM) in different concentrations, sodium chloride (0.9%), DMSO (1% and 0.1% as solvent), and cDDP (10⁻⁴mol/L Cisplatin) with the cells A2780 (left), CalSens (middle) and HEK293 (right).

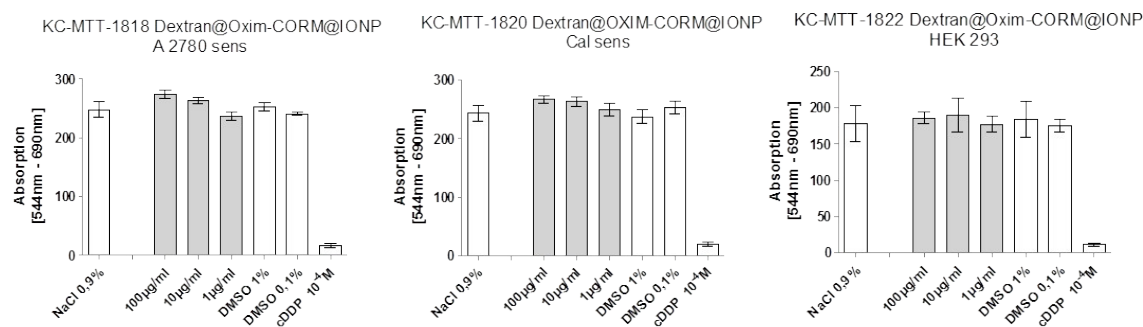


Fig. S38: Toxicity test of dextran@oximeCORM@IONP (**18**) (here labeled Dextran@Oxim-CORM@IONP) in different concentrations, sodium chloride (0.9%), DMSO (1% and 0.1% as solvent), and cDDP (10⁻⁴mol/L Cisplatin) with the cells A2780 (left), CalSens (middle) and HEK293 (right).

Determination of the activation energy for the CO release from oximeCORMs

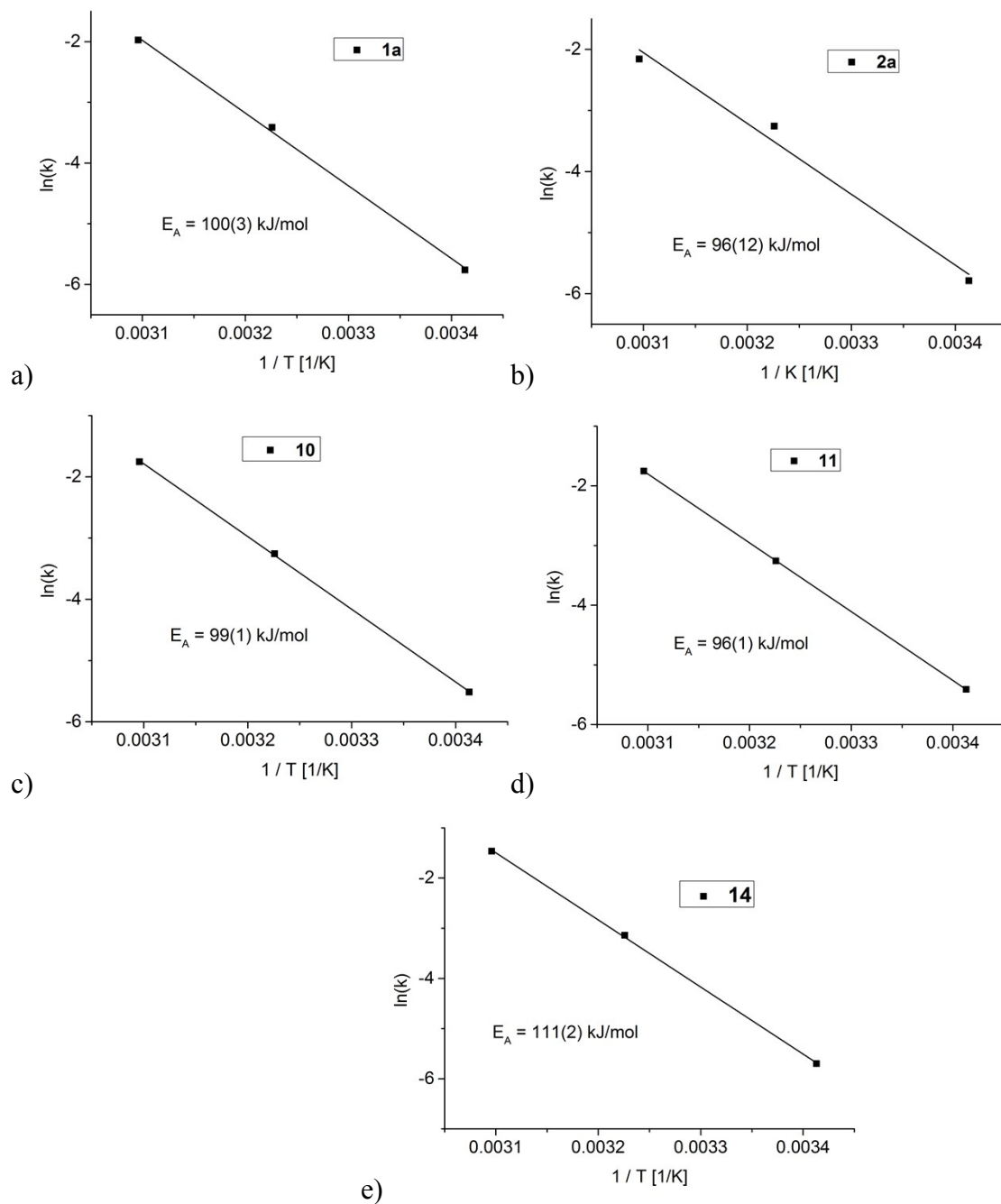


Fig. S39: Arrhenius plot of $\ln k = \ln((\ln 2)/(t_{1/2}))$ versus $1/T_{\text{Kelvin}}$ to determine the activation energy from the slope ($-E_A/R$, $R = 8.314 \text{ J mol}^{-1} \text{ K}^{-1}$) of the graph. a) **1a** b) **2a** c) **10** d) **11** and e) **14**.

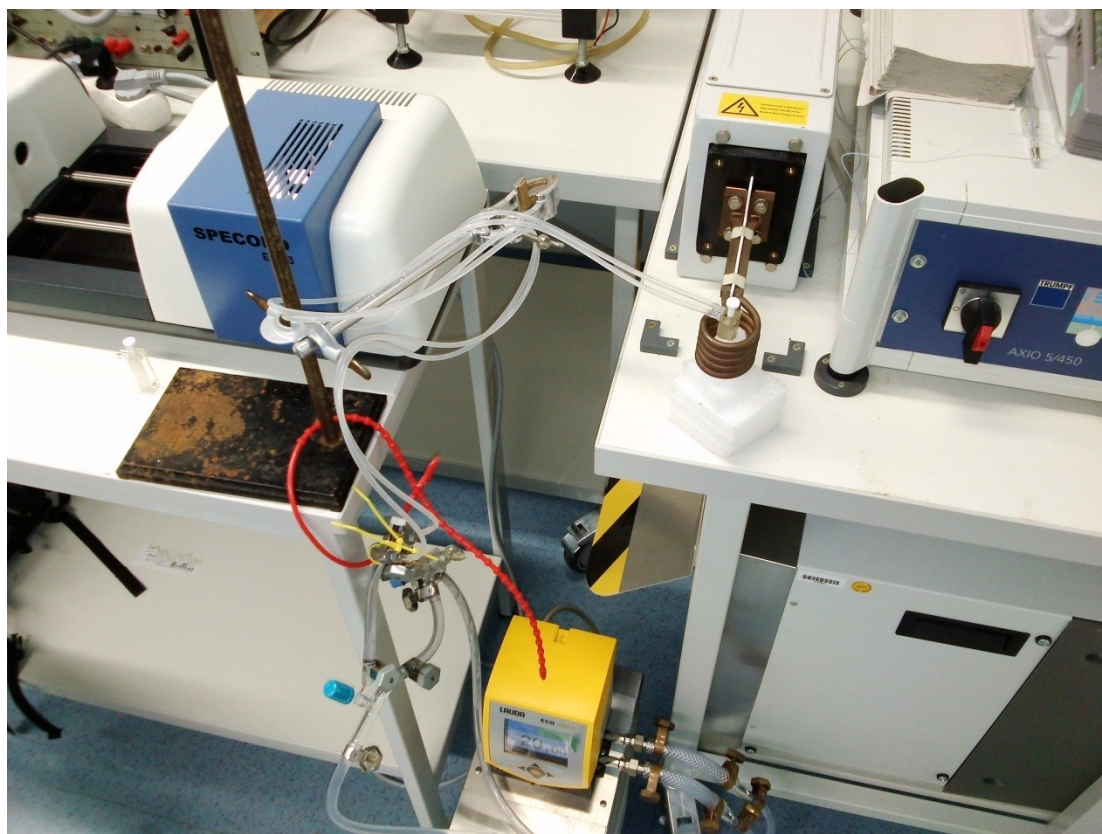


Fig. S40 Setup of the CO release measurements in alternating current (AC) field with a Hüttinger HF generator AXIO T5 and the thermostated quartz cell placed inside the water-cooled copper induction coil.

Literature

- 1 L. Oresmaa, H. Kotikoski, M. Haukka, J. Salminen, O. Oksala, E. Pohjala, E. Moilanen, H. Vapaatalo, P. Vainiotalo, P. Aulaskari, *J. Med. Chem.* 2005, **48**, 4231.
- 2 A. Mantovani, S. Cenini, *Inorg. Synth.* 1976, **16**, 51.
- 3 A. J. Atkin, J. M. Lynam, B. E. Moulton, P. Sawle, R. Motterlini, N. M. Boyle, N. M. *Dalton Trans.* 2011, **40**, 5755–5761.
- 4 E. Neuse, *Met.-Based Drugs*, 2008, 1–19.
- 5 H. Meyer, F. Winkler, P. Kunz, A. M. Schmidt, A. Hamacher, M. U. Kassack and C. Janiak, *Inorg. Chem.*, **2015**, 54 (23), 11236–11246.